Review

Harvesting circuits for triboelectric nanogenerators for wearable applications

David Macário,[1,3,*] Ismael Domingos,[2,*] Nuno Carvalho,[1,3,*] Pedro Pinho,[1,3,*] and Helena Alves[2,*]

SUMMARY

Internet of Things (IoT) and recently Internet of Nano Things (IoNT) bear the promise of new devices able to communicate and assist our daily lives toward wearable technologies which demand a versatile integration such as in wireless body networks (WBN), sensing, and health monitorization. These must comply with stringent constraints on energy usage. Dimensions and complexity intensify the need for small and maintenance-free power sources. Environment energy harvesting and storage is an important approach to sustain operation for a long time. Triboelectric nanogenerators (TENGs) arise as a strong and promising solution to power the new field of outcoming self-sustainable devices, implantable, and wearable devices. They can transform mechanical energy in different modes, have simple structures, and use vulgar and sustainable materials. This paper makes a review about TENGs technology, construction, materials, operation, and focus on strategies for harvesting circuits. Main challenges like efficiency, reliability, energy storage, and sustainability are discussed.

INTRODUCTION

In modern society, prospects of interconnection and advances of electronic integration allow people and services to be more linked together. The idea of interactive objects gives rise to an emerging era of smart objects, smart homes, and even smart cities. All the surrounding individual devices present a unique identity in the digital world by means of the Internet of Things (IoT). Incorporation of nano-scaled devices allows communication through embedded networks at a level of integration that can be particularly relevant in medical applications because data can be extracted *in situ* places previously inaccessible due to bulky sensor sizes, allowing critical biological data communication.

To enable information networks, energy supply has become a critical challenge. Reliable, safe, and affordable power sources are normally required and achieved through non-renewable energy storage units such as lithium batteries. These pose some constraints as they require frequent recharging associated with a limited lifetime and a difficult or often impracticable replacement. Moreover, damaged cells and degradation over a large number of charge cycles contribute to potential pollution of the environment.

Sustainable energy harvesting techniques arise as an alternative to mitigate some of these drawbacks. These can be coupled with conventional battery-based systems and managed to assist and prolong reliable operation (Prauzek et al., 2018). Alternative energy sources include mechanical, thermal, indoor light or sun radiation, electromagnetic waves, or even hybrid systems collecting several forms of stimulus. Among them, mechanical energy is one of the most versatile and can produce a daily power in the order of milliwatts or a few watts in some cases when related to the human body (Zhou et al., 2018a; Wu et al., 2019). This amount of energy, if efficiently harvested, could be sufficient for small IoT/IoNT, wearable or medical devices, sensors, and actuators (Zhou et al., 2018a; Wu et al., 2019; Pu et al., 2018; Xi et al., 2017).

Some emerging technologies are able to generate electrical energy using all these mechanical stimuli in our day-to-day life taking advantage of the triboelectric effect. Already, in the 19th century generators such as the Wimshurst machine and Van de Graaff generator could built-up a high potential through static charge accumulation between two materials. Only later, in 2012, by coupling this triboelectric effect and electrostatic induction at a small scale, a novel nanotechnology introduced by Z.L. Wang group (Fan et al., 2012a) led to a new device generation, the triboelectric nanogenerators (TENG). It takes advantage of low cost, lightweight, easy fabrication, potential ambient friendship, and design as well as the ability to

[1]Electronic, Telecommunications and Informatics Department, University of Aveiro, Portugal

[2]Physics and Chemistry Department, CICECO, University of Aveiro, Portugal

[3]IT, Instituto de Telecomunicações, Aveiro, Portugal

*Correspondence:
alves.helena@ua.pt (H.A.),
dmacario@ua.pt (D.M.),
ismael.domingos@ua.pt (I.D.),
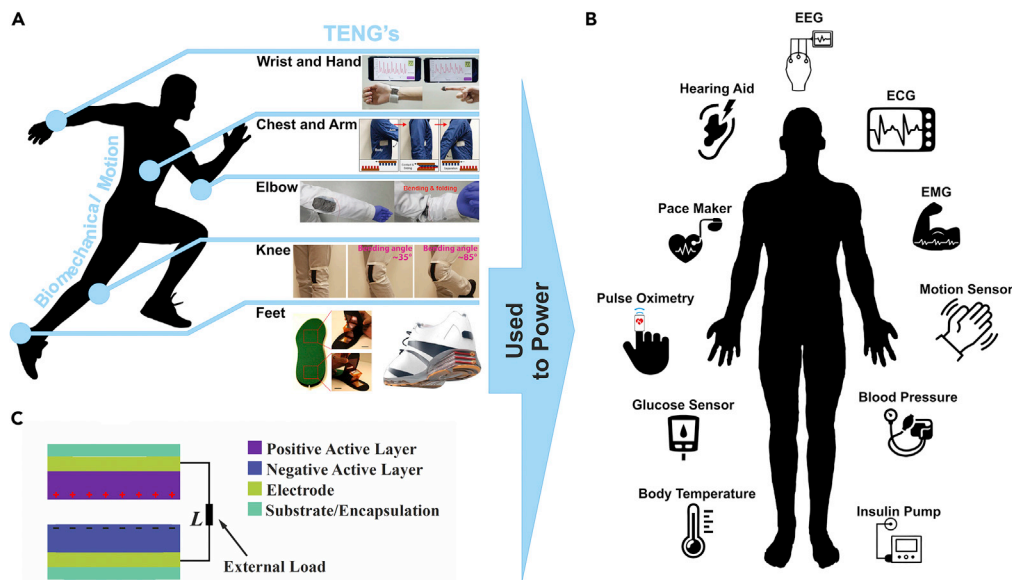nbcarvalho@ua.pt (N.C.),
ptpinho@ua.pt (P.P.)
https://doi.org/10.1016/j.isci.2022.103977

Figure 1. Triboelectric nanogerators concept
(A and B) Biomechanical motion that can be used as energy sources for triboelectric generators (A) and potential applications (B). Adapted from (Fan et al., 2020; Pyo et al., 2020; Hwang et al., 2020; Yi et al., 2015; Niu et al., 2015; Zhu et al., 2013a).
(C) Example of a triboelectric nanogenerator with all the essential components, positive and negative triboelectric layers (triboelectric pair), electrodes and an external load.

provide high voltages owing to their ultra-low capacitance (Zhou et al., 2018b). These can be made in extremely thin, attachable, flexible, and stretchable devices for integration in wearable smart systems. For the last decade, TENGs have been expanding to different fields of applications, acting on stimuli from all kinds of mechanical sources, and ranging from ocean tides (Bai et al., 2019) and wind (Wang et al., 2015b; Chen et al., 2018a) to biomechanical motion (Lou et al., 2020; Liu et al., 2020). The latter is particularly important for wearable applications and takes advantage of movement as walking or running as shown in Figure 1A. In this area, common harvesting devices are applied on movable zones or parts of the body, as wrists and hands to harness energy from moving fingers or hand motion (Alam et al., 2020; Fan et al., 2020). Other moveable parts of the body are also used like the torso while moving the arms (Pyo et al., 2020; Pu et al., 2016b; Zou et al., 2019a), elbows and knees through bending and stretching (Hwang et al., 2020; Yi et al., 2015), and also feet, usually integrating devices on shoe soles to gather energy from repeated stepping (Niu et al., 2015; Zhu et al., 2013a; Shi et al., 2019). TENGs can be considered safer because their output currents are usually in microampere level, which is not harmful to human beings. This fact allowed this technology to expand also to other types of applications such as sensors and implantable devices, either as dermal implants (Li et al., 2020) or directly implanted in organs (Cheng et al., 2020; Ouyang et al., 2019). In addition, TENGs can also be used as active sensors correlating the detailed mechanical motion and output electrical signals (Wang et al., 2015a). Applications such as heart rate monitoring (Lin et al., 2017), movement sensing (Yu et al., 2017a), and tactile sensing (Zhu et al., 2014b) can be effectively and accurately achieved. Moreover, stretchable approaches can be used to allow complete integration in systems as wireless body area networks (WBAN) that rely on full wearable sensor networks to monitor human health as illustrated in Figure 1B.

Some quite encouraging results have already been found with examples of energy harvesting systems based on stretchable and shape-adaptive devices capable of working as energy harvesters as well as self-powered biomechanical sensors. This approach allowed achieving 50.49 $\mu W/cm^2$ of power in just 8 × 4 cm of area using human body motion like in fingers movement (Cao et al., 2020). In another approach, a self-powered motion monitor through integrated shoe-pads was capable of producing 3.375 mW/cm^2 during running activity (Wu et al., 2021). It is even possible to achieve higher generated power, as demonstrated by Xian Li et al. (Li and Sun, 2017) in an experimental wearable harvesting system based on a TENG (9 × 9 cm) that can produce 4.8 mW to power 190 LEDs.

Electrically, TENGs can be treated as a serial connection of a capacitor and an ideal voltage source. Because this output is characterized by low and non-constant currents, it requires an energy storage component to enable stable output to feed an operating device even when the harvester is not feeding enough power. This is usually achieved using capacitors instead of batteries due to their superiority in terms of life cycle and compactness. However, a direct connection between these two is usually not possible and requires energy management circuitry. A main issue is that the output of TENG is also in the form of alternating current (Wang et al., 2015a). Direct current output is desired to supply electronic systems and, therefore, a system that provides AC–DC conversion is required, usually using a rectifier stage.

Over the past years, great efforts have been paid to manage the electrical power generated by TENGs at circuit level. Topologies have been made more complex to mitigate more and more aspects that arise as obstacles to device miniaturization. Even though TENGs are capable of producing high voltages by simply connecting an external capacitor, the output voltage can be lowered and therefore the output voltage of a rectifier will always be less than the maximum input voltage, which may be too low to supply any electronics system. This can be greatly enhanced via voltage multiplier circuits (Zhang et al., 2018; Ghaffarinejad et al., 2018). To optimize the extracted power from TENGs, alternative and more complex strategies for the harvesting circuit are needed. A DC-DC boost converter can be implemented normally based on switched circuits using switched-inductor (SI) or switched-capacitor (SC) topologies. Inductors are suitable for high power applications but require bulky components also presenting reduced scalability (Seeman et al., 2010). For low-power low-area applications, capacitor-based converters are a better alternative because they can be fully on-chip integrated and used for a voltage gain higher than one (Ballo et al., 2019; Ballo, 2020; Ballo and Grasso, 2019; Ballo et al., 2020).

Other approaches rely on charge pumps where charge transfer between the TENG intrinsic capacitor and external capacitors increase the output power. Conventional topologies are known as Dickson and Cockcroft-Walton charge pumps, which use MOSFET diodes and capacitors. Impedance match and voltage regulation between the generator and the final load are also important issues to optimize harvesting systems based on TENGs.

In this review, different working approaches of TENGs have been systematically summarized and analyzed. The paper firstly reviews the basis of its principle, materials, and modification methods as well as different configuration designs and work. After, an overview on harvesting circuits for energy optimization where different approaches and electronic techniques are presented for integration in TENGs to optimize their performance. Finally, challenges and future research trends in triboelectric harvesting of environmental energy are summarized at the end of the review.

TRIBOELECTRIC NANOGENERATORS

These devices rely on the triboelectricity between two dissimilar layers, denominated the triboelectric pair, and in electrostatic induction. Even though TENGs can be designed in several different ways and adapted to many applications, the basic working mechanism is the repeated contact between the triboelectric layers, which will maintain an electrostatic charge generation at their interface. This charge cannot be all collected because it will be the key for the electrostatic induction on the device, therefore, at least one of the triboelectric layers must be a dielectric. Apart from the triboelectric layers, electrodes are also important to connect the device to an external load and ensure charge flow using electrostatic induction.

A common device configuration is depicted in Figure 1C. However, device performance will strongly depend on several parameters as the materials used, their interaction, and even the way triboelectric layers come into contact.

Triboelectric concept

The triboelectric effect is a type of contact-induced electrification, yet there is no full understanding of all the fundamental aspects for this process (Wang, 2013). It is believed that when two materials come into contact, charge transfer occurs between the molecules to equalize the electrochemical potential. Differences in stability, work function, and electron affinity could explain the phenomenon, reflecting on an electron, molecules, or even ion exchange (Diaz and Felix-Navarro, 2004; McCarty and Whitesides, 2008). It is known that the charge exchange depends on several parameters such as temperature, humidity, applied force, and material combination (Xu et al., 2018b).

Almost all materials are capable of creating this phenomenon, be it wood, polymers, metals, or silk, and be used as friction layers in TENGs (Lee et al., 2017). Even though material combinations are countless, not all assemblies will present adequate voltage, current, and power density performance. The charge separation is strongly dependent on the materials' polarity difference, and weak charge separation will result in a low output. In order to be analyzed in a comparable way, this characteristic is usually expressed as a list of materials arranged according to their capability to attract or repel electrons (Wang, 2013). This list is called the triboelectric series and was first published by Johan Carl Wilcke and later complemented by John Henniker (Zou et al., 2019b; Yu et al., 2019). Even though information has grown throughout the years, a compiled series with all existing materials has not yet been attempted due to their large amount and difficult adequate testing approaches. Instead, short lists with the most commonly used materials such as metals and polymers are frequently used as reference, and other focus on specific material such as for 2D layered materials, by Seol et al.(Seol et al., 2018), or polymeric fibers from S. Liu et al.(Liu et al., 2018).

Unfortunately, triboelectric series are only qualitative and do not allow a direct quantitative comparison and reliable conclusion. Efforts have been made for a more replicable method such as the tribo-charger set created by Park et al. to measure charge density from particles through a charge-to-mass ratio of waste plastics. However, this method is only applicable on powder materials, not being able to quantify surface charge density of general flat materials (Park et al., 2008). Recently, Lee and Orr tested surface-to-surface forces in some flat materials to evaluate the effective charge affinity. Their work revealed some incoherencies on most common triboelectric series, usually related to air polarity or to positioning on the list for some materials because most studies are based on chemical electronic affinity and not in the effective electrostatic charge. Unfortunately, this systematic study was only performed on a small number of materials and due to their planar and rigid characteristics, revealed to be highly dependent on surface roughness and applied pressure (Zou et al., 2019b). Zou et al. conducted a study where standardized measurements were performed with a liquid metal as reference, taking advantage of its softness and shape adaptability. This overcame the roughness limitation and was made in a glove-box environment under well-controlled temperature, pressure, and humidity conditions. However, it was still a very selective study in very specific conditions, and therefore, it will demand more efforts with broader situations to characterize all these materials in a standardized and comparable manner.

Dielectric materials

Even though these materials are typically characterized by their electrostatic response, there are other properties still relevant for triboelectric characterization, such as their conductivity. Negative triboelectric layers or electron attractive materials are often purely dielectric polymers such as polydimethylsiloxane (PDMS), polyimide, or silicon rubber due to their high electronegativity. Materials with fluorine functional groups also tend to have high electron attraction, due to very high electron affinity of fluorine. Most common examples of devices that exhibit high conversion efficiency and output power use fluorinated materials as the electron acceptor material, such as polytetrafluoroethylene (PTFE), fluorinated ethylene propylene (FEP), perfluoroalkoxy alkane (PFA), or polyvinyldifluoride (PVDF) (Yoon et al., 2018). In some approaches, these materials are used as the starting layer, on top of which other are deposited, in a bottom up strategy, being most of the times used in the form of films (Bai et al., 2013a; Guo et al., 2015; Jing et al., 2014). In other cases, it is necessary to deposit them on top of a substrate, using liquid processing techniques such as drop cast or spin coating so they can conform to the surface during polymerization (Niu et al., 2014b; Li et al., 2015; Hou et al., 2013a).

Similarly, certain materials are also typically selected as the electron donor or positive triboelectric layers. The most common materials are polymers as polyurethane and polymethyl methacrylate (PMMA) or even common substances as textiles, such as nylon, cotton, or silk. They can be used as thick films, specially PMMA, or thin films as starting layer (Li et al., 2015; Wang et al., 2014a), but solution techniques can also be used to process this kind of materials (Jung et al., 2014; Zhu et al., 2012). In textile applications, it is common to use the fabric as a substrate (Zhou et al., 2014; Cui et al., 2015) or fibers, which later can be knitted (Gong et al., 2017; Yu et al., 2017b; Zhu et al., 2016).

Conductive materials

In the case of conductive triboelectric layers, they are normally used as positive layers and can also be used as electrodes at the same time for connection with external circuitry. They are also important for optimal performance, as they are responsible for charge flow. Hence, if they present low carrier mobility or low

free carrier density, it will lead to a considerable energy loss. This approach integrates metals as aluminum, copper, nickel, or silver as triboelectric layer (Zhu et al., 2013a; Bai et al., 2013a; Lin et al., 2014). These are commonly applied as foils or prefabricated films attached to adjacent layers through adhesion, which is the easiest and cheapest approach to attach this type of layers with high electrical conductivity (Wang et al., 2012; Zhang et al., 2013a). However, it presents some limitations such as low stretchability and breathability. For more reliable, flexible, and controlled layers, it is also possible to use other conventional techniques like physical vapor deposition as e-beam or sputtering even though they are limited to some substrates (Hou et al., 2013b; Zhu et al., 2013b; Bai et al., 2013b; Yang et al., 2013).

Other alternatives have also been tested using carbon-based materials, such as carbon nanotubes or graphene, which offer excellent performance under harsh mechanical deformation or even conductive textiles (Haque et al., 2018; Khan et al., 2017; Tian et al., 2018; Domingos et al., 2021). Mainly targeting applications in fabric, they also offer compatible processing deposition with textiles. Most common approaches use commercial carbon materials processed as inks using solution techniques as drop cast or dip coating. Alternative strategies employing chemical vapor deposition or fibers, in a weaving process, have also been attempted (Zhu et al., 2016; Khan et al., 2017; Ren et al., 2018; Cao et al., 2018; Yang et al., 2018).

Nowadays, conductive polymers, as poly-(3,4-ethylene dioxythiophene) (PEDOT), are well explored due to an easy processing, flexibility, and environmental stability. These attributes make them promising for triboelectric nanogenerators because they can be processed by low-cost conventional solution methods (He et al., 2019).

Surface modification strategies

Regardless of the chosen material, an important aspect that will greatly affect the device performance is the contact area. To increase contact area and boost efficiency, surface patterning is one of the most used strategy. An approach is to perform *in situ* polymerization on top of an already patterned template or mold with microstructures as pillars, pyramids, or domes (Hou et al., 2013a; Wang et al., 2012; Liu et al., 2016), which conform to these structures and result in a patterned triboelectric layer to use on a device. As mold materials, the typical choice is silicon, usually patterned by conventional photolithography methods. Other approaches directly pattern the triboelectric layer, resulting normally in structures as nanowires or nanopores. These are frequently produced using dry etching techniques as reactive ion etching (Zhu et al., 2012; Wang et al., 2013), or wet techniques as electrochemical anodization (Zhu et al., 2013a; Bai et al., 2013b).

The use of additives, such as nanoparticles, to increase the surface area has also been tested. Usually, they are made of the same material, dispersed in a solution, and then casted on the surface (Zhu et al., 2013b; Yang et al., 2013). These kinds of structures can result in output optimization as demonstrated by X. Zhang et al. (Zhang et al., 2013b) where a patterned PDMS film revealed an optimization on open-circuit voltage and short-circuit current by 118% and 61.4%, respectively.

Efficiency can also be optimized through surface modification by chemical processes, by adding other functional compounds that promote higher charge separation. Plasma treatments that add fluorinated groups, raises the electronegativity of the triboelectric material (Chu et al., 2016; Shin et al., 2018). They can also add doping agents (Wen et al., 2018; Fang et al., 2017) or induce ionization (Wang et al., 2014b). Self-assembled monolayers that bond with the surface (Song et al., 2015; Kim et al., 2017; Wang et al., 2016) are also a promising strategy. In the case of D. Shin et al. (Shin et al., 2018), by fluorination in SF6 plasma, the electronegativity of the triboelectric material increased, resulting in an optimization of the open-circuit voltage in 461% and of the short-circuit current in 208%.

WORKING MODES AND CURRENT APPLICATIONS
TENGs are mainly divided into two categories

Dielectric-to-dielectric and conductor-to-dielectric types (Niu et al., 2013b). In the early developments, most devices used purely insulating materials as active triboelectric layers with additional electrodes as depicted in Figure 2A. In this topology, called dielectric-to-dielectric configuration, both dielectric layers acquire an electric charge when rubbed together, maintained during device operation.

An alternative layout in which one of the active layers is a conductive material acting simultaneously as a triboelectric and an electrode layer is called conductor-to-dielectric. This has only one dielectric layer,
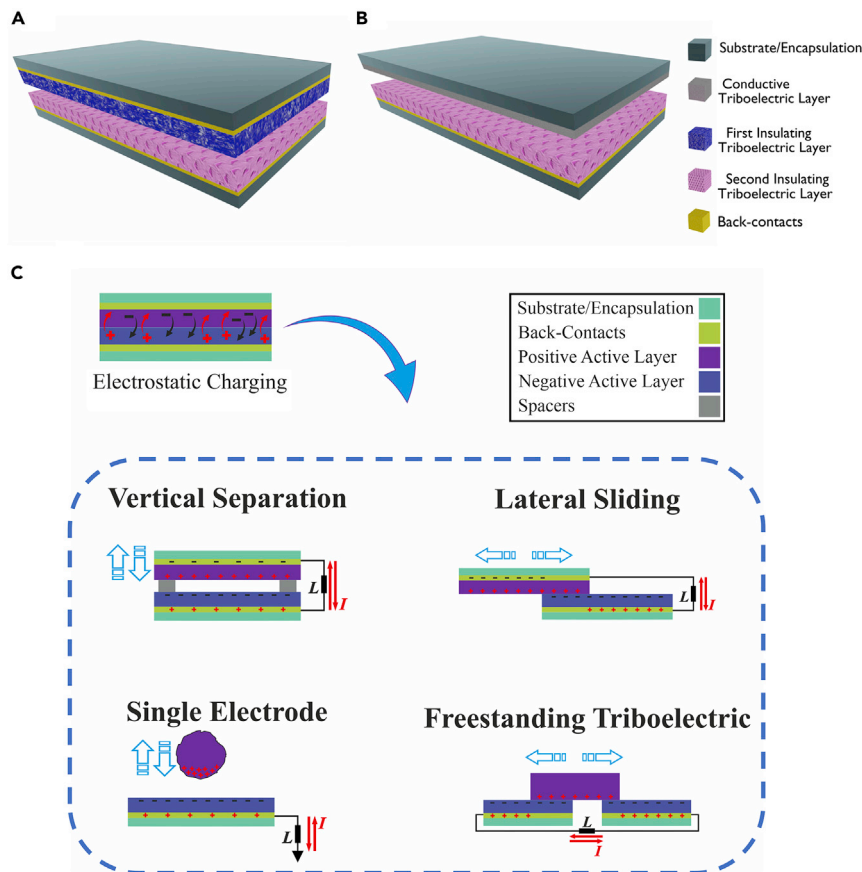
Figure 2. TENGs configuration and working modes
(A and B) Triboelectric nanogenerator in conductor-to-dielectric (A) and dielectric-to-dielectric (B) configuration, with one dielectric active layer paired with a conductive active layer and with two distinct dielectric active layers, respectively.
(C) Four main working principles for triboelectric nanogenerators.

as shown in Figure 2B. Here, the triboelectric effect will occur between the dielectric and the conductive layer. Both layers will be charged, however, charges on the surface of the metallic component are not static, they move and are used to feed an external circuit if electrically connected. Besides the advantage of material saving as well as fewer steps to create a working device, this alternative presents a more efficient charge transfer, resulting in a 57% optimization on short-current transferred charges and 27% on the open-circuit voltage (Niu et al., 2014b).

Even though a conductor-to-dielectric configuration is more advantageous for high-output power nanogenerators, it also presents some downsides. One of the most relevant is the long-time stability, due to reactivity of the metal layer with atmospheric water, which easily oxidizes. The dielectric-to-dielectric approach is more thermally and chemically stable because the insulating layers do not suffer from corrosion and protect the conductive layers from this effect. This allows integration and makes it a valuable material for durable large-scale nanogenerators (Wu et al., 2016).

Triboelectric nanogenerators can present different architectures, which can be divided into four main working modes shown in Figure 2C, which influence the device performance. TENGs can be in vertical contact-separation mode (VS), lateral sliding mode (LS), single-electrode mode (SE), and freestanding triboelectric mode (FS), adaptable to almost all applications (Hinchet et al., 2015; Wang, 2014). Vertical contact-separation mode was the first to be intensively studied for operational triboelectric harvesters and still represents the most popular architecture. This is due to its simplicity and easy adaptation to any movements that depends on a cyclic motion (Wang et al., 2012; Fan et al., 2012b). Lateral sliding mode and single-electrode mode were developed in 2013. The first is based in a parallel motion of triboelectric layers extracting

CellPress
OPEN ACCESS

power mainly from friction. This mode allows better performances and more power generation due to more effective charge separation (Chen et al., 2019). Surface patterning, such as stripes, can be used to increase the number of cycles happening simultaneously in a single movement (Yang et al., 2013; Hinchet et al., 2015; Guo et al., 2016). Single electrode offers the advantage of requiring only one electrode, which is important to overcome limitations associated to VS and LS modes when triboelectric elements need to be free and detached from the external circuit. The FS mode possesses similar characteristics to the SE mode, also capable to interact with several freely moving objects. However, this type of triboelectric harvesters allows enhanced power outputs, taking advantage of a larger active area and material interaction.

On all working modes, the mechanism is similar. After an initial charging of the triboelectric layers through contact, when triboelectric layers come into full contact, electrostatic charges are balanced and total accumulation is established in the interface between triboelectric layers. Upon layer separation, the potential between the electrodes increases and is compensated by charges from the external circuitry, generating an electric current. The charges flow until the triboelectric layers are far enough so there will be no more interaction between their surface charges. This equilibrium is disturbed when an external force is again applied and forces both layers together. This weakens the induction force in each electrode and drives the charges between electrodes, creating an electrical current until the layers come into contact, leading to the starting position. The cycle repetition generates an alternate current in the external circuitry.

Strategy of working-mode applications

All working modes can be engineered and adapted to an intended purpose; the choice usually relies on the ease of implementation and the working mechanism. VS modes are usually associated to material performance studies, surface treatment studies, and simple overall characterization. This is due to its simpler and easier analyze of the physics of the energy harvesting process and more control of contact areas. The same strategy can be used in LS mode, resulting sometimes in better performances but always requiring more complex devices and more integration difficulties. For this reason, it is not common to see lateral sliding mode devices for TENGs, and the FS variation is preferred. FS presents the advantage of all the sliding benefits without the electrical connection constraints between moving layers, in much easier device integration. All these TENG's modes can be applied as energy harvesting devices, as well the single electrode working mode. This last mode is very much used in sensors due to its simplicity and easy integration but normally presents low electrical output. For better comparison and analysis of TENG's working modes in wearable applications, the main characteristics are summarized in Tables 1 and 2.

So far, there is no evidence of a correlation between a specific working mode presenting a superior electrical performance for energy harvesting. As this technology is rather recent, there is still a lot of effort in understanding and characterization materials and overall devices. Therefore, without a standard characterization method transversal to all materials and working mechanisms, different studies tend to test under different conditions such as diverse contact area, external force, frequency, or even computation rules. This limits an overall comparison and reaching to conclusions such as evaluating if a new device exhibits a performance breakthrough.

None of the less, it is already possible to present the main advantages of this technology toward a similar, but more mature technology, such as piezoelectric nanogenerators. Main benefits of TENGs rely on easier and cost-effective fabrication process and materials. Both technologies were proved viable and capable of providing stable power as shown in Figure 3.

TENG's output performance is already comparable to piezoelectric nanogenerators in terms of output power density, and even presents slightly better open-circuit voltages. However, piezoelectric devices require specific materials that display piezoelectric properties while the triboelectric effect is applicable for nearly all materials. Therefore, it is of utmost relevance to refer that with easy fabrication, low-cost materials, and more development regarding characterization and performance optimization it is possible to bring TENGs to a competing level with energy harvesters on current market.

HARVESTING CIRCUITS FOR TRIBOELECTRIC NANOGENERATORS

TENGs cannot normally power the final appliances directly. Therefore, a big effort is needed to design efficient, small, and reliable harvesting circuits for TENGs and maximize the usable energy. Limitations arise as the documented efficiency of the TENGs is low, some of the best results reported are below 50% (Li and

Table 1. Output values and main characteristics of triboelectric nanogenerators for wearable harvesting systems

Wearable triboelectric nanogenerators

	Working mode	Size	Triboelectric pair	Force	Load	Voltage	Current	Power density
Gong et al. (2017)	VS	–	Nylon VS Silicon rubber	100% tensile strain @ 0.5 Hz	500 MΩ	4 V	50 nA/cm^2	0.13 μW/cm^2
Liu et al. (2016)	VS	5 cm × 5 cm × 8 mm	PDMS VS PET	100N @ 1Hz	1 GΩ	500 V	20 μA	15.38 μW/cm^2
Guo et al. (2016)	VS	3 × 3 cm	PET VS Fluoroalklsilanes-PDMS	1.8 Hz	100 MΩ	590 V	12.6 μA	280 μW/cm^2
Ko et al. (2015)	VS	6 × 2.5 cm	PET VS PDMS	39 N @ 0.5 Hz	1 MΩ	8.12 V	26.57 nA/cm^2	125 μW/cm^2
Dong et al. (2017a)	VS	4.5 × 4 cm	Stainless Steel-Polyester VS PDMS	3 Hz	132 MΩ	45 V	0.35 μA	26.34 μW/cm^2
Cheng et al. (2017)	VS	4 cm in length	PDMS-Ag VS PTFE	0.16 N @ 1 Hz	50 MΩ	0.66 V	15 nA	2.25 nW/cm^2
Ouyang et al. (2019)	VS	–	Aluminum VS PTFE	40N @ 1Hz	100 MΩ	97.5V	10.1 μA	11 μW/cm^2
Cao et al. (2020)	SE	8 × 4 cm	Si Rubber VS Skin	Hand tapping @ 2 Hz	50 MΩ	300 V	5.5 uA	50.49 μW/cm^2
Wu et al. (2021)	SE	8 × 8 cm	Skin VS PDMS Foam	10 N @ 5 Hz	–	78.7 V	26.5 uA	3.375 mW/cm^2
Shi et al. (2016)	SE	3 × 3 cm	Multi-wall carbon nanotubes VS PTFE	friction frequency is 10 Hz	100 MΩ	200 V	0.143 μA/cm^2	12 μW/cm^2
Shi et al. (2017)	SE	16 cm^2	Ag VS Cloth	–	700 MΩ	220 V	612 nA	3.75 μW/cm^2
Zhang et al. (2017)	SE	7 × 4 cm	Skin VS PDMS	–	–	45.6 V	25.8 nA	0.09 μW/cm^2
Lai et al. (2017)	SE	16.5 × 11.4 cm	Skin VS Silicon Rubber	6 N @ 1 Hz	1 MΩ	200 V	200 μA	70 μW/cm^2
Zou et al. (2019a)	FS	10 × 6 cm	Water VS Silicon	50% tensile strength @ 1 Hz	300 MΩ	10 V	35.5 nA	6.25 nW/cm^2
Jiang et al. (2020)	FS	28.3 cm^2	Aluminum VS PTFE	@ 1 Hz	5MΩ	51.5 V	2.5 μA	1.42 μW/cm^2
Guan et al. (2021)	FS	5 × 5 cm	PA66 & P(VDF-TrFE) VS Rubber	200N @ 3Hz	10MΩ	166 V	8.5 uA	9.3 μW/cm^2
Pu et al. (2016a)	FS	10 × 10 cm	Ni & Parylene VS Cotton	5 Hz	–	40 V	5 μA	2.42 mW/cm^2
Tian et al. (2017)	FS	5 × 5 cm	Ni & Silicon Rubber VS Skin	300 N @ 3 Hz	10 MΩ	540 V	140 μA	0.892 mW/cm^2

Table 2. Existing methods of power management for TENGs

Methods of power management

Section	Method	Advantages	Limitations
Charge boosting	Cycles for maximized energy output	Increases energy by at least 4 times, being highly significant for small load resistances. Allows extraction of maximal energy output with lower matched impedance. Suitable for pulsed-TENGs	Switch activation control is not always easy to implement. Generated voltages can reach harmful values for switching components
	Charge pumping	Allows very high surface charge density without the need for switching system. Enable stable and ultrahigh power generation in IoT power applications	Demands higher structurally complex TENGs, inefficient for modes with low capacitance variation. Requires additional rectifier systems
AC-DC conversion	Passive rectification	Simple approach of obtaining a high-performance full-wave rectifier configuration and higher efficiency with diodes made from MOSFETS in cross coupling configuration	The main source of power losses within full-wave rectifiers is the diodes' forward voltage drop (≈ 700 mV in Si junction diodes) and the leakage current when the devices are reverse biased
	Active rectification	Higher efficiency by reducing the diodes' conduction losses. Power conversion efficiency can reach 80%–85% with input voltages typically greater than ± 2 Vpk	The control circuitry of active topologies presents additional power consumption and may require conditioned supply which limits TENG miniaturization
Voltage regulation	Bennet's doubler	A simple and compact method for voltage multiplication, obtaining a rectified voltage at the output	Only does voltage multiplication without stabilization and the voltage drop in the diodes directly affects the efficiency
	Switched inductor converters	Allows almost all TENG generated charge to be extracted	Output voltage without stabilization
	DC-DC switched mode converters	The most efficient way to dynamically obtain voltage regulation with buck, boost, and buck–boost configurations	More complex and needs a quiescent power consumption

Sun, 2017), in most cases are around 25%. For practical use of TENGs, improvements are needed to rise to the maximum the efficiency on the harvesting circuits employed. For that, power conditioning circuits using TENGs need to provide very efficient rectification and storage of the incoming AC power, while drawing as little quiescent current as possible. Additionally, power stabilization and adequate level shifting of the output voltage may be required.

For now, miniature TENGs with less than 100 cm^2 can produce some milliwatts of power (Wu et al., 2019; Li and Sun, 2017). This reduced amount of power is due to the reduced amount of free energy to harvest, and the poor efficiency of the generators, with less than 50% of the available mechanical energy transformed in electrical energy. So, the overall efficiency of the electronics that transform the electrical energy produced by the TENG in useful energy for the load is critical for practical applications of TENGs (Szarka et al., 2012).

A basic diagram of an energy harvesting system can be seen in Figure 4A. The architecture is divided in four blocks, the generator "TENG", the "Energy conditioning" block (includes impedance match, rectification, and voltage regulation/stabilization), energy storage, and the final load (Kong et al., 2010; Tabesh and Fréchette, 2010; Qiu et al., 2009).

The energy conditioner normally reduces output voltage to the appropriate value for the final application. The storage unit stocks electrical energy for future exploitation, normally using supercapacitors or batteries, and to provide stable energy output. "Load" is the end user of the electric power harvested. In IoT and
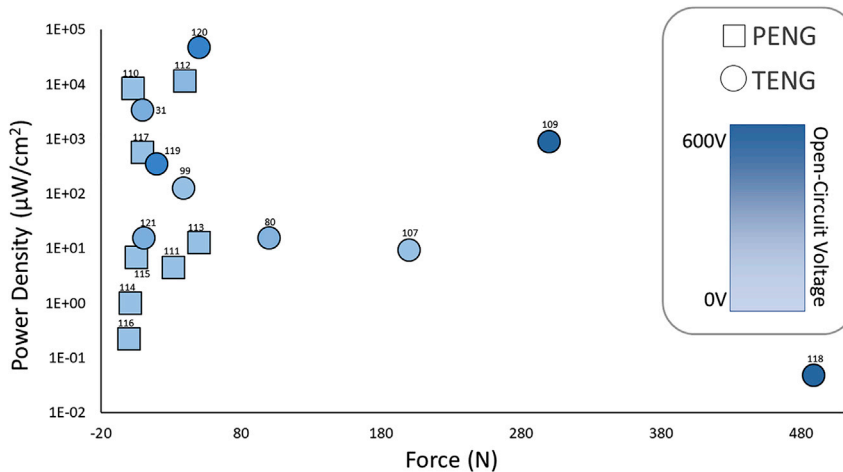
Figure 3. TENGs versus PENGs performance

Graphical comparison between several piezoelectric nanogenerators (PENG) based on different materials as cellulose (Pusty and Shirage, 2020), PVDF (Bhavanasi et al., 2016; Ye et al., 2019; Chen et al., 2017; Dudem et al., 2018; Yu et al., 2016), PET (Kang et al., 2017), or PDMS(Maria Joseph Raj et al., 2019) along with some of the previously cited TENG devices incorporating materials as PVDF (Guan et al., 2021; Soin et al., 2016), PDMS(Wu et al., 2021; Liu et al., 2016; Ko et al., 2015; Chun et al., 2016; Wang et al., 2020a), PVC(Feng et al., 2021), or silicon rubber (Tian et al., 2017). Output performances are presented in terms of power density according to the necessary applied force for device operation. Additionally, the gradual color shift (light to dark blue) is associated to the device open-circuit voltage, showing higher values for TENG devices.

wearable applications, these are usually devices that operate on a transient basis, spending the rest of the time in a latent or low power mode.

TENGs are basically an electrostatic generator with very high impedance; they produce very low current at relative high voltages. Taking as an optimistic example a TENG with 4.8 mW of peak output power at 70 V, the peak output current will be only 69 μA (Li and Sun, 2017).

To optimize the energy transfer from the generator, impedance match is essential. Nonlinear techniques, which use switched circuits to adjust the harvesting circuit to the oscillation frequency of the generator SSH (Synchronized Switch Harvesting) (Viallet and Cedex, 2006) or algorithms such as MPPT (Maximum Power Point Tracking) using low-power processors (Qiu et al., 2009).

There are applications where the device to be powered consumes more energy than the harvesting system can collect and conditioning. In this case, if the load does not run continuously, and the average consumption is equal to or less than what can be harvested, it is possible to feed these devices as long as energy storage elements are included in the energy conditioner. Used as backup to the generator, these storage elements can have a great impact on the applicability of the harvesting circuits.

Electric model of a TENG

The electrical model of a TENG is presented on Figure 4B. The most important theoretical equation for representing the real-time power generation of a TENG, Equation 1, is a relationship among three parameters: the voltage (V) between the two electrodes, the amount of transferred charge (Q), and the separation distance (x) between the two triboelectric charged layers, which can be named the V-Q-x relationship. The open circuit voltage (V_{OC}) and the capacitance (C_{TENG}) are only functions of the moving distance (x) and are structural parameters independent of motion parameters, such as velocity and acceleration (Niu et al., 2014a). The equivalent circuit model of TENG can be derived from their governing equation (V-Q-x relationship) (Niu et al., 2013b; Niu et al., 2013a; Cheng, 2019), as shown in Equation 1,

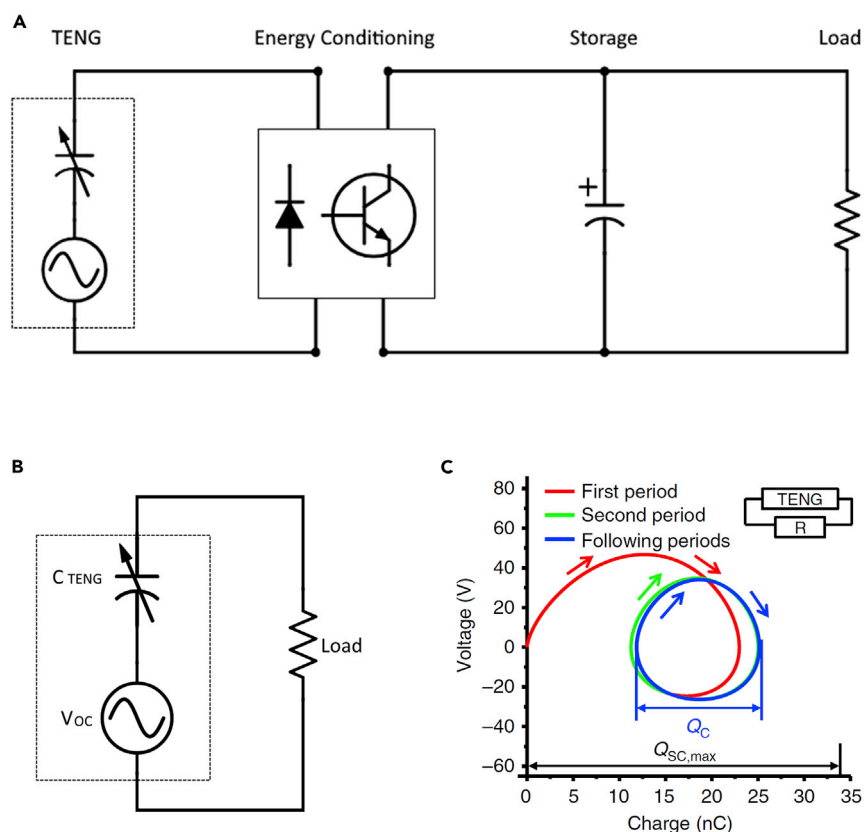$$V = -\frac{1}{C_{TENG}(x)}Q + V_{OC}(x)$$

(Equation 1)

Figure 4. TENGs electrical modeling

(A–C) (A) Harvesting system block diagram, (B) electrical model of a TENG, (C) demonstration of the V-Q plot, adapted from (Zi et al., 2015).

In this expression, the first term is originated from the capacitance between the two electrodes and can be represented by a capacitor. The other term is originated from the separation of the polarized tribo-charges and can be represented by an ideal voltage source. The simplest equivalent circuit model is shown in Figure 4B. The inherent capacitance of TENG will show impedance to the AC signal from V_{OC}. Any structural parameters that increase the capacitance will lower the impedance of the TENG and thus lower the matched load impedance. An increase in body vibrations is equivalent to increase in the frequency of the AC signal of V_{OC}; so, the matched impedance will also be lower (Niu et al., 2014a).

With this simple model, a simulator of an entire TENG system can be built by integrating the TENG equivalent circuit model into a circuit design software (any SPICE simulator like LTspice) in order to assist the development of conditioning circuits (Ghaffarinejad et al., 2018). This implementation can be based in analytical derivation of the referred terms and, as it depends on structural parameters, it will vary according to the geometry and working mode of the TENG. C_{TENG} and V_{OC} are described by different equations for different operating modes (Niu and Wang, 2014). The effectiveness of this model was validated by Niu et al. (Niu et al., 2014a), using a simulator with analytical solutions of the equations that govern some TENG systems.

As an alternative, Hinchet et al. (Hinchet et al., 2018) used a finite element method calculation in Multiphysics. The results were very similar, with an error lower than 3%. The model was experimentally tested, using a TENG which was simulated and validated in laboratory, and found good consistency between simulation and experimental measurements.

To measure experimentally C_{TENG} and V_{OC}, a reference work was presented by Lu et al. where they used a setup where the AC signal Vac is applied in series with TENG, together with a resistor (Lu et al., 2016). By

detecting the phase difference of the signals on TENG's two nodes, its capacitance can be measured dynamically with the device mounted on a shaker at an average acceleration equivalent to most common uses. This procedure provides the device capacitance variation, ΔC_{TENG}, and thus the maximum and minimum values of C_{TENG} ($C_{TENGmax}$, $C_{TENGmin}$), used to calculate V_{OC}.

Along with these fundamental characteristics, a standard figure of merit (FoM) is essential for performance evaluation of power management circuits. Two distinct analyses can be performed. A resistive analysis approach allows to observe the output power behavior, relating the peak point with the device inherent impedance. Alternatively, using a capacitive analysis approach is possible to evaluate charge transferred by the device and accumulated on the load. In this case, the peak of storage energy is associated with the TENG inherent capacitance (Niu and Wang, 2014).

A common approach to evaluate TENGs' performance quantitatively is to use the average output power as an estimative for the standard FoM. However, a comparison based on generated energy per cycle can provide a better evaluation of TENG operation, has been recently preferred as FoM. This method was proposed by Zi et al. and known as the built-up voltage-transferred charge plot, or as the V-Q plot (Zi et al., 2015). An example can be seen in Figure 4C, highlighting that the cycles energy only stabilizes after a couple of periods, which needs to be accounted while evaluating and comparing TENG's performance. This is valid for a device coupled with a certain load resistance. Under different load resistances, the steady-state cycles behave differently, revealing mainly transferred charges at higher loads and mainly high voltages at lower loads.

The principle behind the V-Q method is that the generated energy per steady-state cycle E, under a time interval T, is given by:

$$E = \underline{P}\,T = \int_0^T VIdt = \int_{t=0}^{t=T} Vdq = \oint VdQ \qquad \text{(Equation 2)}$$

Where Q is the transferred charge between electrodes. Using Equation 2, it is possible to quantify the energy per cycle and correspond to the enclosed area in the plot. In extreme cases, such as mainly transferred charges or mainly high voltages, this resulting area is nearly null. Between these two extremes, a certain load resistance results in a larger enclosed area and, consequently, a higher energy output per cycle. Similarly, to a transferred power distribution, this resistance value is closest to the TENG inherent impedance under the tested conditions. Therefore, FoM allows to extract relevant information related to device intrinsic properties as well as evaluate the energy characteristic of its working cycle.

TENG charge boosting strategies
Cycles for maximized energy output
After analysis of a typical V-Q plot, it is possible to observe that both charge and voltage never achieve its maximum values, corresponding to transferred charge under short-circuit conditions and open-circuit voltages, respectively. This happens due to a static connected load which cannot be null for short-circuit conditions and at the same time infinite in an open-circuit state, and therefore will only favor one of these parameters. Consequently, the theoretical maximum energy per cycle will not be achieved. To optimize this problem, a method was proposed by Zi et al. to achieve maximized energy output during each stable cycle (Zi et al., 2015). This approach relies on a switch connected with the load which is controlled by the voltage peak on the device. It activates whenever maximum or minimum voltage is achieved during the repeated cycles, which are directly related with larger energy output values. The dynamic control will commute the device between a short circuit and an open-circuit state, extracting the maximum charge from the TENG. When the switch is connected in parallel with the load, it will allow a short-circuit path on the device. Therefore, maximum energy output per cycle is achieved for an infinite resistance load because it will control the open-circuit state.

In typical electronic devices, lower resistance loads are present, and these will not be able to provide open-circuit conditions. To overcome this problem, the switch is applied between the TENG and the load to optimize output performance. Using this strategy, the switch will force an open-circuit state when open and allow a low resistance path through the load when closed. The main limitation of this method lies in the switch activation control. The easiest solution usually relies on assigning this control to the displacement of the triboelectric layers in the device. However, the relation between these mechanical characteristics

and the relevant voltage peaks is not always simple. Additional problems related with switch implementation can arise because typical TENG generated voltages can reach 2.5 kV, which are harmful for regular electronic components.

Charge pumping

An additional fundamental parameter that needs to be considered is the charge density in triboelectric layers. This will directly influence characteristic values, as open-circuit voltage and transferred charge, affecting the energy output per cycle. Charge density enhancement is limited by the triboelectrification ability of the triboelectric pair associated with the surface topography and by the discharge induced by air breakdown. In typical TENGs at ambient conditions, the maximum charge density is around 250 mC m^{-2} (Cheng et al., 2019). This can be optimized in a high-vacuum environment, reaching up to 1003 μC m^{-2}, but it requires complicated device packaging (Wang et al., 2017). To mitigate this problem, some approaches arise based on charge pumping through integrated charge excitation. Liu et al. (Liu et al., 2019) proposed a system based on charge transfer between the TENG intrinsic capacitor and external capacitors, with the charges being directly excited on the electrodes depicted in Figure 5A. This way, an external or self-excitation system supplies the main generator to create a sustainable and stronger electric field, thereby producing a stable and higher output power.

In this case of an external system, the produced AC signal must be first rectified to a DC output excitation voltage. This is injected into the TENG during contact state to increase the power generation. When the two electrodes separate, these charges are transferred from the main TENG back to a charge storage capacitor. During repeated cycles, these will flow back and forth between the storage capacitor and main TENG to achieve an optimized output performance. On a self-excitation system, the charge transfer occurs between the main capacitor and an external capacitor. This external capacitor will be responsible for the output excitation voltage but will be fed directly by the main TENG rather than by an external source. Both these capacitors will be connected with the main TENG and an automatic switch between parallel and serial configuration will dictate when the excitation is applied to the device (Liu et al., 2019).

Using this external charge excitation system with a 5-μm thick dielectric, it was possible to reach an effective charge density of 1.25 mC m^{-2} (Liu et al., 2019), 1.24 times higher than the previous highest value obtained with a similar configuration, depicted in Figure 5B (Xu et al., 2018a). In self-excitation systems, the charge accumulation is faster, reaching a saturation state within only 50 s at 1 Hz. However, it achieves a slightly lower power density of 35.9 W m^{-2} when compared to an external excitation with a power density of 38.2 W m^{-2}.

Both these examples enable stable and ultrahigh power generation in large-scale power applications. Nonetheless, these approaches are designed for TENGs that present high capacitance variation. This characteristic is common in contact-mode devices with relatively low dielectric layer thickness but is not frequently observed in rotation and sliding mode.

The first example of a charge pumping technique to boost the output performance of sliding TENGs was recently proposed by Bai et al. (Bai et al., 2020). In this approach, illustrated in Figure 5C, bound charges are injected directly from a pumping TENG into the main device through a synchronous rotation structure. This stacking design allowed to implement multiple main TENGs supplied solely by one pumping TENG. In this approach, the AC output produced by the pumping TENG is converted into a DC voltage and injected into an active layer. Because this was designed to apply on a freestanding triboelectric mode, the excitation voltage is applied on the freestanding layer.

When compared to a normal rotary-disk TENG with a similar structure and the same contact area, this technology results in an increase of charge density by a factor of 9, under the same drive frequency. It also shows results regarding average power, 15 times higher than a normal device (Bai et al., 2020). However, this method is only suitable for rotation and sliding-mode TENGs, being associated with a considerably high current leakage into the system. Nevertheless, this charge pumping strategy provides a promising approach to obtain a high-power output in low-frequency mechanical energy harvesting and should influence the design of high-output TENGs and their practical application in different areas.
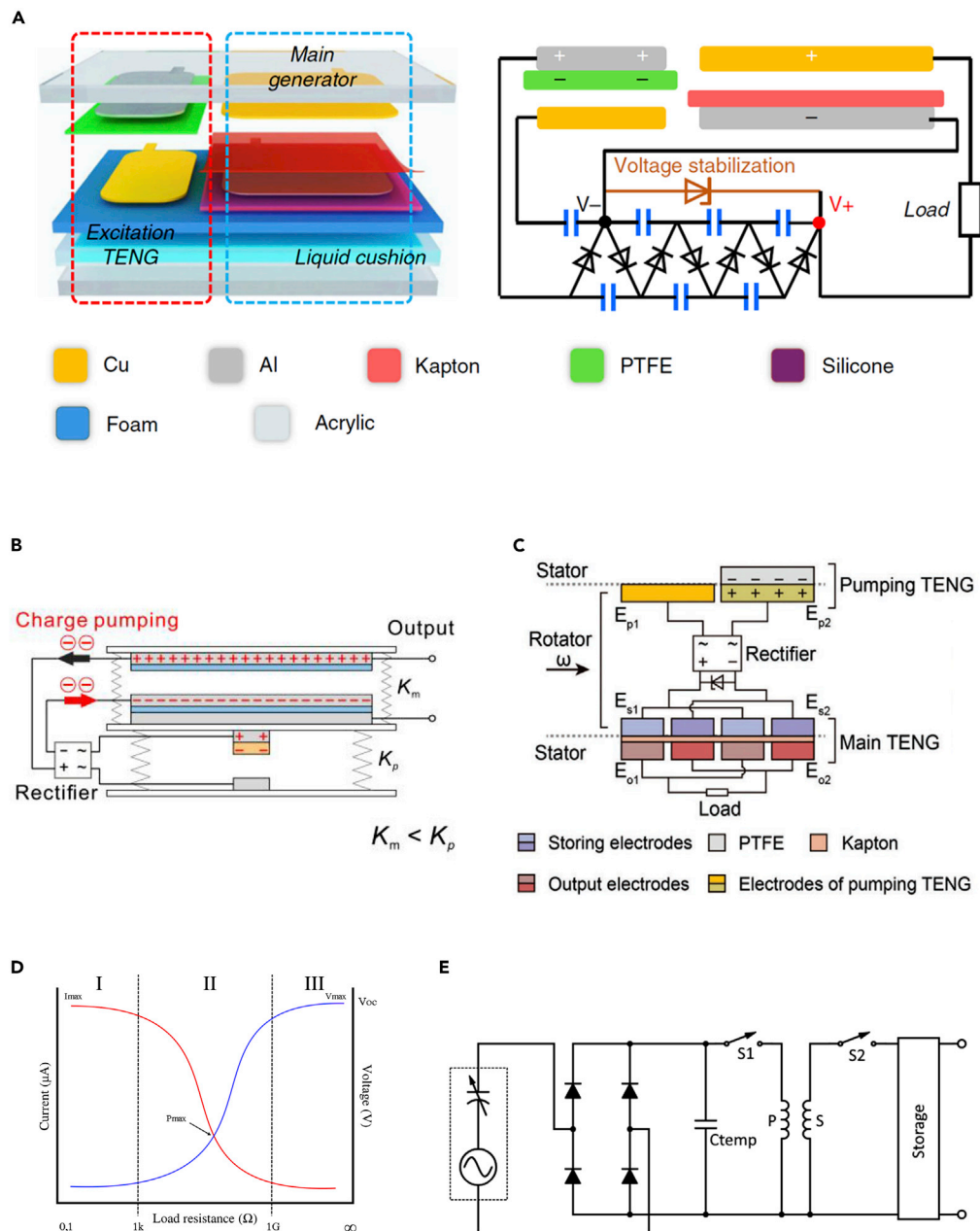
Figure 5. Charge pumping systems and impedance matching

(A–D) (A and B) Structural illustration of external charge excitation triboelectric nanogenerators accompanied by the schematic of the associated electric circuit, adapted from (Liu et al., 2019; Xu et al., 2018a), (C) Illustration and schematic for circuit connection of a rotary charge pumping triboelectric nanogenerator, adapted from (Bai et al., 2020), (D) Illustration of the three working regions when a TENG is connected to a resistive load. Adapted from (Cheng, 2019).

(E) Switched resonant transformer circuit (Niu et al., 2015).

Impedance matching

TENGs' output characteristics are high voltage and very low current, leading to a very high impedance, typically tens to hundreds of mega-ohms (Niu et al., 2013b; Niu et al., 2013a; Niu and Wang, 2014; Hinchet et al., 2018).

TENG connected to resistive load

The operation of a TENG connected to a resistive load can be divided into three working regions (Niu et al., 2013b; Niu et al., 2013a; Niu and Wang, 2014), as shown in Figure 5D. Region I has low load resistance (0.1Ω to 1kΩ), where the peak value of output current has dropped a little from the short-circuit state, the maximum voltage is low nearly proportional to the load resistance. In this region, TENG behaves like a current source. In Region II, with an intermediate load resistance (about 1kΩ to 1GΩ), the maximum current decreases with the rise of resistance, while the voltage increases. In this transitional region, the TENG transfers its maximum power to the load. In Region III, load resistance values are larger than 1GΩ, and TENG behaves like a voltage source, with a saturation of the maximum voltage at characteristic generator V_{OC} (see the TENG model in Figure 4B). In this region, like in region I, the extracted power is lower than region II.

TENG connected to capacitive load

TENG has an inherent capacitance, represented by the variable capacitor C_{TENG}. This capacitance is usually very small leading to a high output impedance of the TENG when collecting energy from vibrational mechanical energy like human movements.

A study to optimize a capacitive load impedance matching with a specific TENG was presented by Simiao Niu et al.(Niu and Wang, 2014). They conclude that the maximum power transfer is obtained when charging a load capacitor equal to the intrinsic capacitance, C_{TENG}. Considering the capacitance of an energy harvesting unit larger (in the microfarad level) than C_{TENG}, the charging efficiency for the energy storage can be severely affected and therefore it is an important issue to address.

TENG impedance matching with inductive transformer

TENGs can be adapted to the electronics of the power management unit using an inductive transformer. This approach shows the advantage of reducing the voltage as well as the matched impedance, resulting in higher current and power transfer efficiency. However, the transformer has a central frequency band where it is more efficient, and out of this region the efficiency of the transformer dramatically decreases. The inductive transformer is more convenient in situations where the TENG collects mechanical energy from a steady high-frequency source. This is the case reported by Guang Zhu et al., where a rotary TENG (19 mW/cm^2) was coupled to the power management circuit composed by a rectifier, a voltage regulator and capacitors through an inductive transformer (Zhu et al., 2014a). The set can deliver a DC output at a constant voltage of 5V in less than 0.5 s after the TEG starts to operate.

TENGs that harvest random mechanical vibrations like human movements can also be adapted using inductive transformers. In this case, the transformer is connected to the TENG using a switched resonant configuration. First, a temporary capacitor (CTEMP) is charged, then the capacitor is switched (S1) to the primary coil of the transformer, optimized to resonate with CTEMP. At an optimum point, S1 opens and the energy transferred from P to S is connected via S2 to be stored, as illustrated in Figure 5E. This solution was presented by Simiao Niu et al. (Niu et al., 2015), to implement an universal charging system based on a TENG.

Conditioning, AC to DC conversion

The output of a TENG generator is AC, which needs to be rectified as most cases stabilized to connected power electronics have a load. Wu et al. presented an experimental example of this approach in a TENG harvesting system with an average output power during slow walking of 7.53 μW (Zhou et al., 2018a). Rectification is a very critical phase for the overall efficiency of the circuit. The simplest option is to use passive rectifiers with Schottky diodes. In this case, the diode voltage drop is not a problem; however, the leakage current can compromise the overall efficiency of the system.

Passive rectification

Passive rectifiers can also be used in different configurations, namely as voltage multipliers, providing some voltage level shift, and is the simplest topology to achieve AC to DC conversion. The full-wave rectifier circuits consisting of four diodes are the most common circuit (Wu et al., 2019; Li and Sun, 2017; Tse et al., 1995), sometimes referred as standard. The main source of power losses within full-wave rectifiers are the diodes' forward voltage drop ($\approx$ 700 mV in Si junction diodes, Figure 6A) and the leakage current when the devices are reverse biased (Rajasekaran et al., 2008). Reducing the forward voltage drop can increase both the power and voltage conversion efficiencies and extend the useful input voltage range of the generator. The use of Schottky barrier
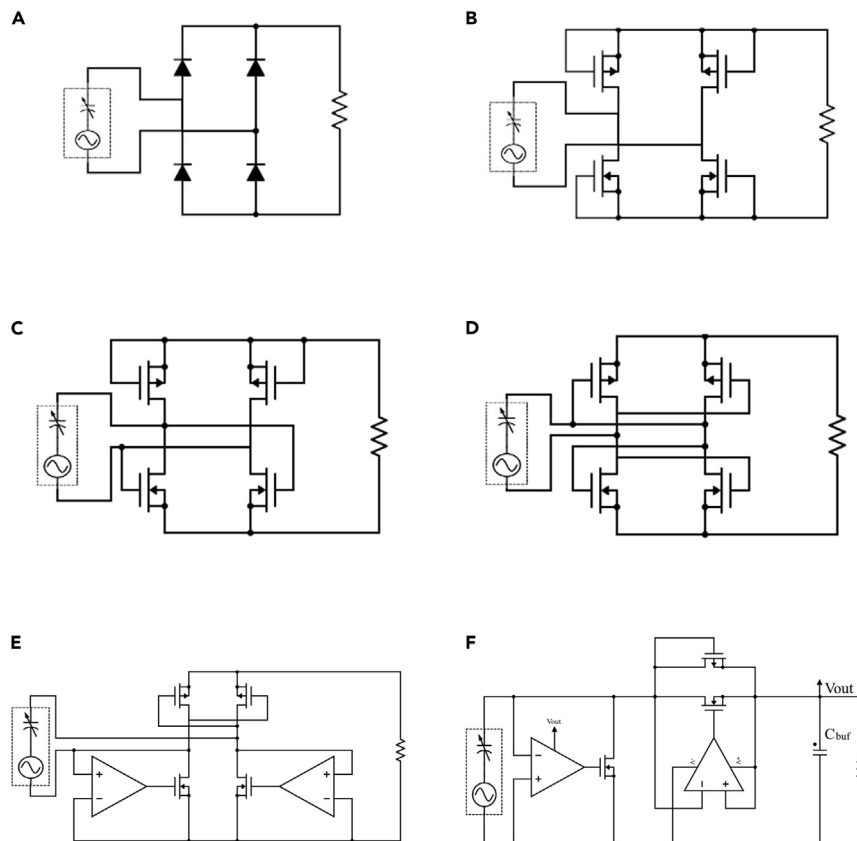
Figure 6. Passive and active full-wave rectifier circuits
(A) Diodes.
(B) Diode-tied MOS rectifier.
(C) Gate cross-coupled NMOS rectifier.
(D) Cross-coupled rectifier.
(E) Active full-wave rectifier with two actively switched and two cross-gate-coupled MOSFETs (Ramadass and Chandrakasan, 2010b).
(F) A self-start enabled synchronous rectifier with a low-power trigger circuit acting as a switch between the energy storage capacitor Vin and a boost converter Vout (Ramadass and Chandrakasan, 2010a)

diodes offer lower voltage drops (ex. BAT43, V_f = 330 mV @ I_f = 2 mA) but at the expense of lower reverse breakdown voltages and increased reverse leakage currents. Moreover, the fabrication costs are higher, as they are not directly compatible with CMOS production processes (Hashemi et al., 2009).

Xian Li et al. successfully managed to achieve a wearable harvesting system using this simple approach. By using a passive bridge rectifier and a filtering capacitor for energy conditioning, the system reached an efficiency of 24% of applied mechanical power versus electrical energy collected (Li and Sun, 2017).

In some integrated circuit designs, the diodes are often replaced by MOSFETs in a diode-tied configuration (Li et al., 2020; Saeid and Aghcheh, 2011). In this configuration, there is no need for an external supply, and the source is permanently shorted to the gate to form a two-terminal device. This is an attempt to improve efficiency, but the sensitive of threshold voltages of the transistors, particularly when the diode-tied MOSFETs are not fully turned ON or OFF (Li et al., 2020), can increase the voltage drop across the devices significantly (Figure 6B). The forward voltage drop can also be reduced in transistor-based passive rectifier designs when the devices are driven directly by the input. For example, Le et al. (Le et al., 2006) reported a passive full-wave rectifier that uses parallel transistor switches (Figure 4C). Different gate cross-coupled topologies are a popular solution for improving the conversion efficiency in integrated MOSFET-based full-bridge rectifiers (Saeid and Aghcheh, 2011). Cross coupling can increase power

conversion efficiency up to 70%–80% even for low input voltages ($\approx 0,8$ V_{PP}), as shown by Hashemi et al. (Hashemi et al., 2009) (Figure 6D).

Despite reducing the voltage drop in the current path under 0.1V, input voltages greater than 1–1.5 V are still essential in order to switch the transistors ON and OFF completely. In order to reduce the threshold voltage, precharged floating gate transistors (Peters et al., 2008) or different biasing (Lam et al., 2006) and bootstrapping circuits (Hu and Min, 2005) can be added to the design.

When the reverse leakage current is the most significant power loss, as in TENG high-voltage output or high-temperature applications, ultra-low-power diode-based rectifiers have been reported to offer a better power efficiency (Rue et al., 2006). These diodes are realized by connecting an NMOS and a PMOS diode-tied MOSFET in series.

Active rectification

Active or synchronous rectifier designs (Clare and Burrow, 2008) can also be used to further increase the efficiency by reducing the conduction losses. However, the control circuitry of active topologies presents additional power consumption and may require conditioned supply which limits TENG miniaturization. The switching devices in synchronous designs are referred to as "active diodes," consisting of a MOSFET driven by a comparator that monitors the transistor's source–drain voltage (Peters et al., 2007). To achieve better conversion efficiencies than passive rectifier topologies, optimization in comparator design is essential. The reported power consumptions for comparators, range from microwatts to nanowatts.

A supply current requirement of 3.3 µA at ± 2.75 V is reported (Peters et al., 2007) to power the comparator, note that this value can compromise the use of this circuits with small TENGs.

Integrated active rectifier topologies are among the most used design. Examples include two actively switched and two cross-gate-coupled MOSFETs. Power conversion efficiencies are reported for input voltages typically greater than ± 2 V_{pk} and can reach 80%–85% (Diaz and Felix-Navarro, 2004), achieving 10–20 mW. In light load conditions, ~ 1 mA at 2 V, voltage conversion efficiency can even reach 95% (McCarty and Whitesides, 2008).

Achieving power conversion efficiencies in the 80%–90% range with active rectification is possible even at power levels as low as 20–30 µW as presented by Le et al (Le et al., 2006). The authors conclude that the synchronous full-wave circuit is more efficient than the passive design. In addition, if a low-voltage threshold process is used, then passive rectifiers could possibly offer superior performance at lower power levels (Lehmann and Moghe, 2005).

Active rectification circuits face the challenge of start up with no previously stored energy on the system. One possible solution is to use active components that can be powered directly from the generator's output (Hashemi et al., 2009; Clare and Burrow, 2008). Alternatively, active circuit designs that can also operate passively can be used. Dallago et al. (Lee et al., 2017) designed a switched-inductor converter that operates as a passive voltage doubler circuit when not actively driven, relying on the parasitic body-drain diode of the MOSFETs. Finally, an additional passive circuitry can also be used to bypass the active parts of the system during start-up (Marinkovic et al., 2009; Xu et al., 2007). The passive circuit can be used to charge the main storage element directly (Marinkovic et al., 2009).

The higher voltage drops of passive start-up circuits place increase minimum voltage requirements on the harvester, which limits the potential miniaturization. In order to reduce the minimum operating voltage needed for a boost converter to start-up, Wu (Sze et al., 2008) proposed a "threshold voltage" start-up scheme, where a combination of the input power and output storage is used to supply the gate-drive block. Ramadass and Chandrakasan (Ramadass and Chandrakasan, 2010a) proposed a solution that starts up at input voltages as low as 35 mV. In this design, a boost converter uses a motion-activated switch driven by the environmental vibrations to achieve an output voltage of 1 V.

Voltage regulation

The output voltage of the energy conditioning circuit must comply with the requirements of the load to be fed by the harvesting system or at least the requirements of the energy storage unit, if used. The required
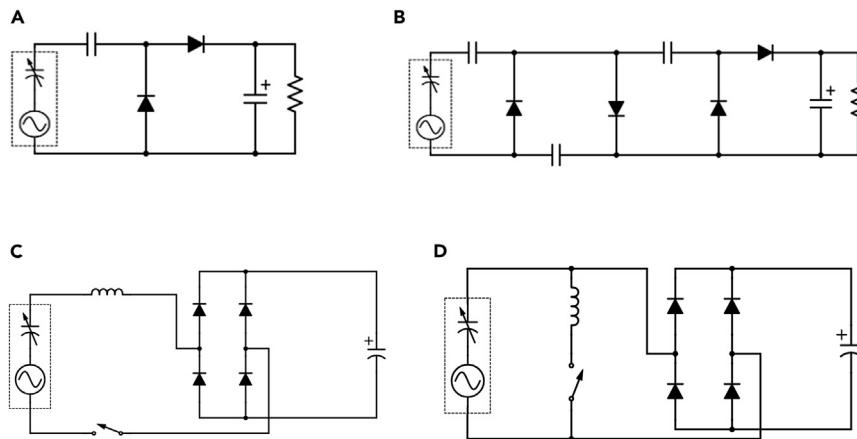
Figure 7. Circuits for voltage regulation
(A) Basic voltage doubler.
(B) Example of a Cockcroft-Walton voltage quadrupler circuit and rectifier, based on passive switched-capacitor principle.
(C and D) Resonant switched-inductor converters, (C) series-SSHI, (D) parallel-SSHI.

voltage rectification, conversion, and regulation can be achieved by using one of two approaches: either by using single-stage circuits as part of the rectification process, or by connecting separate rectification and dc-dc converter stages.

Switched-capacitor converters provide rectification and a degree of voltage conditioning. These self-commutated capacitor converters are often referred to as voltage multipliers, while actively driven topologies are typically referred to as charge pumps.

An example is the n-fold voltage multiplier, which consists of n capacitors and n diodes, or switches, which can be arranged in cascade, and define the converter's properties, such as the voltage and output resistance (Lin and Chua, 1977). There are two main sources of losses within a switched capacitor converter: conduction losses of the semiconductor devices (including losses due to the diodes' forward voltage drop) and charge-up losses within voltage source-capacitor loops (Tse et al., 1995). The losses can be modeled as a series output resistance and are a function of the switching frequency, the number of multiplication stages, and the size of the capacitors used.

A voltage multiplier conditioning circuit for TENG based on the Bennet's doubler was presented by Ali Ghaffarinejad et al (Ghaffarinejad et al., 2018). This circuit uses only diodes as automatic switches to reconfigure the charge-storing capacitors between series and parallel modes Figures 7A and 7B. They investigate the circuit performance in an exponential and unstable mode in comparison with passive half-wave and full-wave rectifiers. The full-wave rectifier shows a better performance during the first 5 s, and the half-wave rectifier between that instant and 32.6 s. From there on, the Bennet's doubler accumulated energy keeps increasing until the diode breakdown voltage is reached, which makes it possible to implement as a charge boosting technique. The maximum voltages are 26, 165, and 835 V (diode breakdown voltage) for the full-wave, half-wave, and Bennet's doubler, respectively. The drawback of this double topology is the very high output voltage, as high as 835 V (Hou et al., 2013a). A solution for the problem, and to make it suitable for low-voltage electronics, is a direct switching of the output voltage, enabling energy storage into a capacitor that drives the load (Hwang et al., 2020). Alternative approaches employ step-down DC-DC buck converters presented below, represented in Figure 8A.

Karim Rawy et al. describe an active-driven circuit energy harvesting system on integrated circuit for a TENG (Rawy et al., 2018). The system utilizes a novel single-comparator-control algorithm to improve the power conversion efficiency. It modulates the switching frequency of the implemented switched capacitor charge pump in proportion to the load condition at a given applied vibration frequency. This allows to regulate the input voltage at the maximum possible power point without IC breakdown. The fabricated test chip in 65-nm CMOS technology achieved a peak power conversion efficiency of 88% with 2.4 μW–15.6 μW input power and power density of 39.59 μW/mm^2.
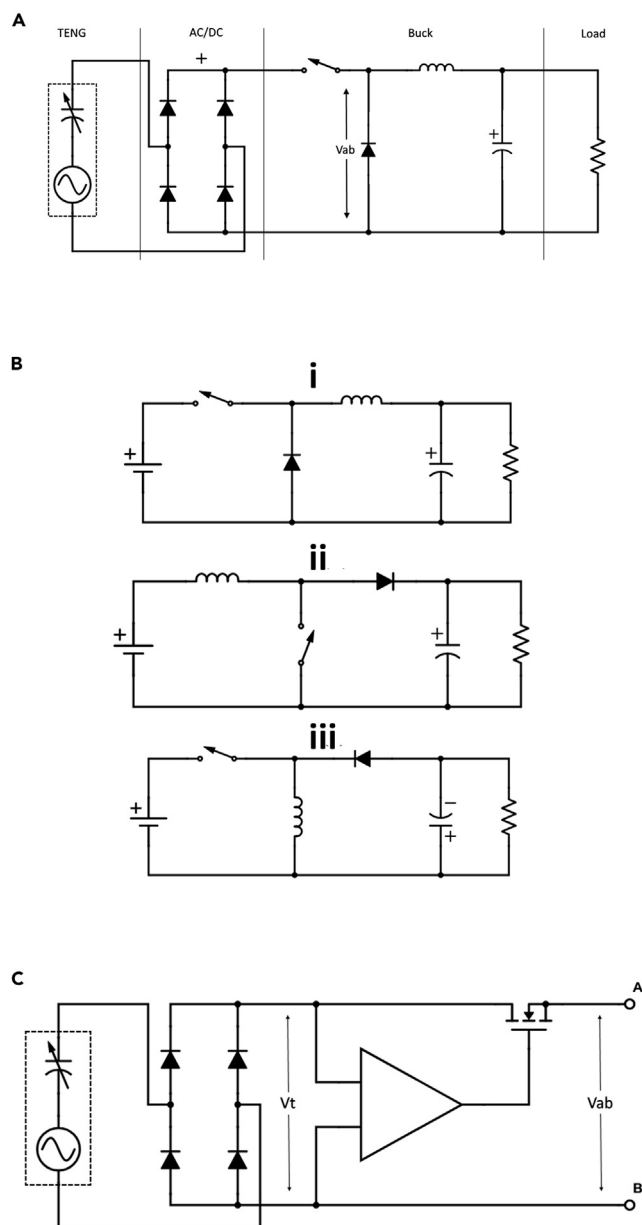
Figure 8. Voltage Buck-boost strategies

(A) Representation of a harvesting system with Buck converter topology (Xi et al., 2017).

(B) DC-DC switched-mode converters, (i) Buck, (ii) Boost, and (iii) Buck–boost configurations.

(C) Self-management switching circuit proposed by Fengben Xi et al., adapted from (Xi et al., 2017).

Switched-inductor converters

An LC resonant rectifier circuit can be formed by using an inductor of typically less than 1 mH (Ramadass and Chandrakasan, 2010b). The added inductance allows almost all generated charge to be extracted, while reducing the losses that are typically associated with a capacitive source charging another capacitor (Zhu et al., 2013a; D'hulst et al., 2005). The topologies shown in Figures 7C and 7D provide an inversion of the voltage at the peak displacement point and thus result in an increase of the harvested power, as shown analytically by Guyomar et al (Marzencki et al., 2008). The first circuit, Figure 7C, is a series-synchronized switch harvesting on inductor (SSHI) and has the inductor connected in series with the generator. A parallel connected inductor is used in the parallel-SSHI, Figure 7D. While the parallel-SSHI circuit maintains the generator connected to the reservoir capacitor via the rectifier block, the series-SSHI remains in open

circuit for most of the cycle, thus allowing the voltage to rise above the reservoir capacitor's voltage. In practice, the voltage inversion, and, therefore, the generator maximum power yield, is limited by the series resistance of the inductor and the voltage drops across the switching devices (Lallart Guyomar, 2008).

A universal self-charging system driven by random biomechanical energy was presented by Simiao Niu et al. (Zhu et al., 2013a). Their power unit can provide a continuous DC output, driven by low-frequency human biomechanical energy. Even if the energy source was random in amplitude and frequency, it was still enough for sustainable operation of various wearable electronic devices, such as temperature sensors, heart rate monitoring devices, pedometers, and wearable watches. The conditioning system, based on a switched inductor principle, can achieve an efficiency of 60% (defined as the ratio of the maximum DC power stored into the storage unit to the maximum AC power delivered to a resistive load).

DC-DC switched-mode converters

The classic switch-mode (switched inductor based) converter topologies, buck (Tabesh and Fréchette, 2010), boost (Carlson et al., 2010), and buck–boost (Lefeuvre et al., 2007) converters have also been evaluated for energy harvesting applications, and demonstrated to provide twice as much output power as linear regulators (Anton et al., 2009), Figure 8B.

Lefeuvre et al. investigated a full-bridge rectifier and a buck–boost converter, driven by a low-power crystal oscillator without an intermediate reservoir capacitor (Lefeuvre et al., 2007). They achieved an 80% efficiency in the range at 1-mW power levels.

A similar peak efficiency, 85%, was obtained by an integrated buck converter design (Ramadass and Chandrakasan, 2010b), designed to regulate the output of a switched-inductor resonant rectifier. This high efficiency was possible at sub-100 μW power levels, thanks to a quiescent power consumption of the control circuitry of around 2 μW.

Microscale energy harvesting applications may require power conditioning circuits that can operate with very low input voltages. The boost converter proposed by Carlson et al. (Carlson et al., 2010) offers a potential solution as it achieves 60%–70% efficiency with input voltages in the range of 50–250 mV at 10–100 μW power levels when connected to a 600-mV supply to drive the switches. Here, the minimum input voltage is just 20 mV with the control circuit consuming only 1 μW of quiescent power.

A universal power management strategy for TENGs, Figure 8C, was proposed by Fengben Xi et al (Xi et al., 2017). They maximized the energy transfer using direct current buck conversion and a self-management mechanism. With the implemented power management module, about 85% energy can be autonomously extracted and output a steady and continuous DC voltage on the load resistance. The first step of the strategy was to maximize the energy transfer from the TENG to the buck converter, as shown in Figure 8A. Although the maximum energy can be transferred from the TENG, the high voltage pulse V_{AB} obtained still cannot directly supply most of current consumer electronics. Voltage regulation was done with a DC-DC buck converter, coupled between the switch and load resistor, a parallel freewheeling diode, a serial inductor and a parallel capacitor are added in sequence. In this case, the switch has two functions, maximize energy transfer and control the DC buck conversion circuit.

To achieve an autonomous TENG switching in the self-management mechanism, without any external power supply, the switch can be controlled by a micro-power voltage comparator and a MOSFET. Driven by the TENG, the comparator is used to compare the rectified voltage with a pre-set reference voltage.

Circuits, qualitative analysis

Energy storage

One significant challenge for small electronic devices is that the energy sources are unable to provide sufficient energy for continuous and long-time operation. Most of the applications where TENGs can be used, the mechanical energy to harvest is not available all the time. For instance, in wearable devices and implants, the human body has different periods and patterns of activity (Zhou et al., 2018a; Li and Sun, 2017). In harvesting systems, energy storage units are very important to guarantee readiness and a stable output of electrical energy to the electronic devices. They can collect the excess of energy that could be

collected in some periods by the generator or satisfy peaks of power when coupled to devices that work periodically like telemetry sensors or small actuators.

Currently, lithium-ion batteries and supercapacitors are widely utilized as the main electrochemical energy storage devices. They can be used as the energy supply units for powering mobile phones, personal wearable devices, microelectronic devices, etc. Supercapacitors are faster to charge and support more charging cycles but by other hand the batteries normally store more energy than supercapacitors.

Rigid power supplies, e.g. coin cell batteries, work perfectly hand-in-hand with classical, rigid electronics. However, to achieve the full potential of wearables and printed electronics, the power source has to be flexible as well. By printing the battery, the power source can be made mechanically flexible and can be freely designed to incorporate just the right amount of energy for the envisioned use-case (Ostfeld et al., 2016; Hu and Sun, 2014; Yang et al., 2020; Wang et al., 2020b). In this regard, the combination of printed and classical electronics to fabricate a hybrid system enables a multitude of opportunities of flexible electronic applications.

Batteries

Batteries store electric energy by electrochemical process. The choice of battery can be approached from many perspectives. The most important factors affecting the choice are application requirements (e.g., need of quick charging/discharging, lifetime, cycling, size, weight, and flexibility).

Important battery specifications include storage technology, energy density, internal resistance, depth of discharge, self-discharge, and tolerance to overcharging (Prauzek et al., 2018). To use with TENGs, the self-discharge and energy density are key requirements. The self-discharge of the battery enters directly in the whole harvesting system efficiency calculations and can compromise this usability.

The energy density (Wh/kg) indicates the maximum density of the stored energy in the battery per unit of mass and differs for individual battery chemistries. The battery capacity is the amount of energy that can be stored in the cell at the full charge. The lifetime of most electrochemical batteries is on the order of hundreds to thousands of charging/discharging cycles. During this time, the battery capacity gradually decreases because of the chemical corrosion of its electrodes. Michal Prauzek et al. present in (Prauzek et al., 2018) a review of the characteristics of batteries for the principal chemistries.

For small applications where rigid batteries can fit, rechargeable Li-Ion batteries are the most used solution. Small commercial button cells with 0.7 g with capacity of 16 mA/h are available in the market.

For wearables, flexible batteries are very interesting approach. Aminy E. Ostfeld presents on (Ostfeld et al., 2016) a flexible battery that consists of printed anode and cathode layers based on graphite and lithium cobalt oxide, respectively, on thin flexible current collectors. It displays energy density of 6.98 mWh/cm^2 and demonstrates capacity retention of 90% at 3C discharge rate and $\approx$99% under 100 charge/discharge cycles and 600 cycles of mechanical flexing. The battery built on this work is used to power a pulse oximeter, demonstrating its effectiveness as a power source for wearable medical devices.

In this field, there are efforts to reduce production cost and environmental impact. Xiao Wang et al. demonstrated on (Wang et al., 2020b) the cost-effective and scalable fabrication of rechargeable printed Zn// MnO_2 planar micro-batteries, with important features of scalability, environmental benignity, high safety, and metal-free current collectors, possessing high volumetric energy density (393 mAh/g), excellent rate capability, and long-life cycling durability. Taking into the full considerations of low-cost and safe Zn, earth-abundant MnO_2, environmentally benign neutral aqueous electrolyte, and inexpensive screen-printing technology, the strategy of constructing printed Zn//MnO_2 MBs holds great potential as next-generation microscale power sources in various wearable, flexible, miniaturized, and printed electronics.

Capacitors and supercapacitors

Another alternative are supercapacitors, which are characterized by high power density compared to common capacitors. A supercapacitor can have a very large capacitance, starting on some Farads in small units, reaching hundreds of Farads. They are constructed either as electrochemical double-layer capacitors (EDLCs) or pseudocapacitors. The first one works on the electrochemical principle. The electric charge is

situated between electrodes with high surface area and thinner electrolytic dielectrics (Chen et al., 2020a; Schneuwly and Gallay, 2000). Their maximum operating voltage is given by the breakdown parameters of the dielectric material. Their rated voltage, normally between 2.5 V and -3′.5 V, includes a safety margin to prevent electrolyte decomposition and subsequent short circuit. Pseudocapacitors have lower power density than EDLC devices, but provide higher specific capacitance and energy density (Prauzek et al., 2018).

The main issue of EDLC is the relatively low energy density. In contrast, the typical energy density of pseudocapacitance can be 100 times higher than that of EDLC, which is beneficial for storage energy (Chen et al., 2020a). In pseudocapacitance, the charge is electrochemically stored through faradaic charge transfer between the electrode and electrolyte, mainly accomplished through three processes, namely underpotential deposition, redox reaction, and intercalation.

Compared to rechargeable batteries, supercapacitors have several advantages (Prauzek et al., 2018) *such as a* fastest charging/discharge process, *or a* large number of charge/discharge cycles without a significant decrease of performance and storage capacity (around 500,000 to 1,000,000 cycles, depending on the manufacturer). Supercapacitors also present a high charge/discharge efficiency (up to 98%) and operate in a wide range of temperatures (between $-40°C$ and $+65°C$ for both EDLC supercapacitors and pseudocapacitors).

A drawback related to the use of supercapacitors in energy harvesting is they self-discharge during the time. This phenomenon is commercially designed as leakage current, a problem related to the terminal voltage of the energy stored in the element (Lewandowski et al., 2013). The magnitude of the problem depends on device capacity, but also differs among manufacturers or even among individual production batches, and normally can reach some micro-amps. Other problem is the shape and rigidity of normal supercapacitors, normally a cylinder shape like a cell or to be soldered in a PCB.

The drawbacks of supercapacitors can at first view compromise the use of supercapacitors as storage devices with TENGs. But there are very interesting experimental developments in the field of flexible, evenly, stretchable supercapacitors applied to harvesting systems (Pu et al., 2016a; Yang et al., 2020; Dong et al., 2017b; Jost et al., 2013). Kai Dong et al. report a highly stretchable and washable all-yarn-based self-charging knitting power textile that enables both biomechanical energy harvesting and simultaneously energy storing by hybridizing a TENG and a supercapacitor into the same fabric (Dong et al., 2017b). They used the weft-knitting technique and special yarns to create a functional textile structure with the TENG and capacitor, elastic, flexible, and stretchable. The knitting TENG fabric is able to generate a maximum instantaneous peak power density of ≈ 85 mW/m^2. The resulting harvesting system uses a conditioning circuit based on a simple full-wave rectifier and demonstrated capability to power small wearable devices.

CHALLENGES AND DISCUSSION FOR ENERGY HARVESTING WITH TENGS

Efficiency and power management

The most limiting problem to the massive use of TENGs is still the output characteristics and power management. Main limitations rely on high open-circuit voltages and low output currents that result in power loss in the subsequent power conditioning circuit. Several methods have been applied to improve the output power such as increasing the number of energy cycles using grid electrodes, reducing the thickness of the dielectric layer, or designing the structure of spacers. In addition, the output power density can be optimized by the mismatch impedance of hybrid generators. Effective power management is crucial to achieve maximum energy transfer during the process of energy storage, management, and transportation. This can be the key point for achieving an effective self-powered functional system. For the design of efficient circuits, there are important improvements and challenges to solve, such as leakage currents and voltage drop in electronic components, and impedance matching, between the generator and the system to be powered. In addition, voltage regulation and stabilization are also key issues as the systems expected to be powered by these generators will need 1 to 5 V. Achieving an efficient energy storage is also important, to have enough energy when there is no mechanical energy to harvest. For practicality and comfort, it is desirable to have reduced dimensions to be portable or easy to wear or implant.

Durability and fatigue

Another issue involves TENG's long-term operation and frequent mechanical stress that can reduce device durability. This is especially relevant when used in flexible and wearable applications as in wireless body

networks. Nanogenerators can be rigid devices, and hard to integrate in a comfortable or easy way on fabric and clothing. Some attempts to overcome these constrains aroused in the form of bottom-up approaches like devices based in triboelectric fibers which are knitted to form a TENG. However, it complies complex processing techniques, which need to be adapted to fabric production methods or to be knitted separately and then patched to the fabric. This kind of devices can be produced with areas of several square cm as the example of Chen et al. with 6.8 × 7 cm and produce high voltages of 4,5k V with currents in the order of 40µA (Chen et al., 2020b). Other alternatives rely on flexible materials such as silicone or elastomers to work as triboelectric layer and encapsulation at the same time and ensure device perseverance in harsh and intensive applications, such as biomechanical energy harvesting. This approach is reliable in bending and deforming conditions but presents limited integration into clothing and textile substrates, and therefore, normally applied directly on bare parts of the body. An example of this is the device produced by Zhang et al. where a device with close to 3 × 3 cm could reach a deformation in the order of 1036% in a stretching motion to produce 92 V and a current of 1.25 µA (Zhang et al., 2020).

Degradation can also occur in harsh environments where dust and moisture can penetrate the layers affecting their reliability and robustness (Zhou et al., 2019; Xu et al., 2019). Attempts to overcome these constrains aroused such as healable polymeric layers that can recover up to 97% in strain after healing broken devices operating for 2 h at 65°C (Xu et al., 2017) or even multi-layered encapsulation to improve the durability and reliability in severe environments (Zheng et al., 2016). Another alternative comprises on using liquid materials instead of solid, reducing the abrasion by frictional contact and diminishing sensitivity to humidity, for example (Cho et al., 2019). Waterproof devices using hydrophobic polymeric layers (Chen et al., 2018b; Yan et al., 2018) have also been considered, as washability is crucial for a successful integration in fashionable garments and power wearables.

Environment and sustainability

Environmental sustainability is also a common problem because some triboelectric materials can be difficult to degrade naturally and can present considerable ecological impact. To improve sustainability, materials more environmentally friendly and degradable materials are considered a priority to achieve green nanogenerators. Materials such as silk and paper can be used as triboelectric layers and lead to biodegradable devices (Guo et al., 2017; Kim et al., 2010). Even though there are several applications of triboelectric nanogenerators targeting wearable electronics, biocompatibility and flexibility for full integration still needs to be developed. Biocompatible materials as polypropylene have been explored as ferroelectret to optimize direct contact with human skin (Li et al., 2016).

Beside experimental field, important work still needs to be done on the research for industrial sustainable processes to mass produce these generators.

CONCLUSIONS

TENGs are a very promising technology to power the new field of outcoming wearables, IoT and IoNT devices. An intense work is ongoing on materials and structures with recent work published in several areas of application. In the generators field, the big challenges are the development of more efficient, reliable, industrial viable, and ambient friendly devices. In this review, TENGs for harvesting environmental energy are summarized considering the material selection, the device structure, and their working principle, followed by recent efforts to enhance the output performance.

Regarding the material choice, there is a great tendency toward low-cost and easy processing materials such as polymers, being mainly accompanied by metallic-based layers to serve as interface with external electronic constituents. This is presented as the preferable approach to study the material interaction as well as the effect of surface optimization. However, in wearable applications, for example, this is expanding into stretchable electrodes to adapt to the mechanical stress these devices need to withstand. This evolution into flexible, stretchable, and transparent technologies is being carried on branching to different working modes in several approaches of implementation, allowing a great versatility for TENGs in this area of application. In the case of implantable devices, the struggle entails the compatibility of materials and their stability in a living and dynamic biological environment, which has been exploited in some examples on literature.

The type of working mode for each case is mainly dictated by the application itself. For wearables, one of the most common to encounter is freestanding mode because it allows for better performances while

interacting with freely moving or even foreign objects. There is also common to find several implementations of TENGs as sensors operating on single-electrode working mode. Even though it is characterized by lower output values, it is more sensible to smaller-scale stimulus, which can be ideal for sensing purposes.

Although there has been a consistent choice of materials for contact surfaces and well-determined working topologies for ease comparison between devices, detailed information regarding material properties, surface treatments, and the way they interact is inexistent and sometimes difficult or impossible to acquire. For this reason, the differences between each case study may be enough to cause a significant variation in the triboelectric properties and complicate reproducibility and reliable comparisons for characterization purposes even though the used structures are rather simple. This is what pushes for the development for a standardized figure of merit for this kind of nanogenerators, which still demands further in-depth investigation.

Owing to the unique features of electrical output of TENGs, such as large impedance, high voltage, and very low current, the electrical power generated by TENGs is hard to be delivered to the load efficiently or stored directly by high-capacity energy storage devices. There are some experimental demonstrations for electronic circuits to condition the electrical energy produced by TENGs, starting with basic approaches based on simple full-wave rectifiers and large capacitors, and going to more efficient and complex circuits with switched circuits and transformers. Fundamentally, there is an intrinsic capacitor inside the TENG that makes it high impedance, high voltage, and low current. Because this intrinsic capacitor is usually very low, the charging efficiency for an energy storage unit, such as a capacitor or a battery, would be very low. The subsequent need for a correct impedance match between the TENG and the energy conditioning circuit. But there is not a well-accepted topology for the harvesting circuit and further work needs to be done. The electric model of TENGs, already obtained, is an essential tool for engineers to develop this work, match the conditioning and storage circuits of the harvesting systems.

The advances made in all these fronts, efficiency, mechanical resistance, bio-compatibility, and sustainability, can lead to substantial progress in the commercialization and implementation of TENG in the industry. Nevertheless, extensive and in-depth studies are still needed to meet the requirements of diverse applications as future self-powered systems or complete wireless body networks.

AUTHOR CONTRIBUTIONS

H.A., P.P., and N.C. conceived the work. I.S. and D.M. carried out the analysis and wrote the manuscript under the co-supervision of P.P. and H.A.

DECLARATION OF INTERESTS

The authors declare no competing financial interests.

REFERENCES

Alam, M.M., Lee, S., Kim, M., Han, K.S., Cao, V.A., and Nah, J. (2020). Ultra-flexible nanofiber-based multifunctional motion sensor. Nano Energy 72. https://doi.org/10.1016/j.nanoen.2020.104672.

Anton, S.R., Erturk, A., Kong, N., Ha, D.S., and Inman, D.J. (2009). Self-charging structures using piezoceramics and thin-film batteries. In Proceedings of the ASME Conference on Smart Materials, Adaptive and Intelligent Systems. SMASIS2009. https://doi.org/10.1115/SMASIS2009-1368.

Bai, Y., Xu, L., Lin, S., Luo, J., Qin, H., Han, K., and Wang, Z.L. (2020). Charge pumping strategy for rotation and sliding type triboelectric nanogenerators. Adv. Energy Mater. 10. https://doi.org/10.1002/aenm.202000605.

Bai, P., Zhu, G., Liu, Y., Chen, J., Jing, Q., Yang, W., Ma, J., Zhang, G., and Wang, Z.L. (2013a). Cylindrical rotating triboelectric nanogenerator. ACS Nano. 7, 6361–6366. https://doi.org/10.1021/nn402491y.

Bai, P., Zhu, G., Lin, Z.H., Jing, Q., Chen, J., Zhang, G., Ma, J., and Wang, Z.L. (2013b). Integrated multilayered triboelectric nanogenerator for harvesting biomechanical energy from human motions. ACS Nano. 7, 3713–3719. https://doi.org/10.1021/nn4007708.

Bai, Y., Xu, L., He, C., Zhu, L., Yang, X., Jiang, T., Nie, J., Zhong, W., and Wang, Z.L. (2019). High-performance triboelectric nanogenerators for self-powered, in-situ and real-time water quality mapping. Nano Energy 66, 104117. https://doi.org/10.1016/j.nanoen.2019.104117.

Ballo, A., and Grasso, A.D. (2019). A simple and effective design strategy to increase power conversion efficiency of linear charge pumps. Int. J. Circuit Theory Appl. 48, 157–161. https://doi.org/10.1002/cta.2704.

Ballo, A., Grasso, A.D., and Palumbo, G. (2019). A review of charge pump topologies for the power

management of IoT nodes. Electron 8. https://doi.org/10.3390/electronics8050480.

Ballo, A., Member, S., Grasso, A.D., Member, S., and Palumbo, G. (2020). Charge pump improvement for energy harvesting applications by node pre-charging 7747, 1–5. https://doi.org/10.1109/TCSII.2020.2991241.

Ballo, A. (2020). Current-mode body-biased switch to increase performance of linear charge pumps. Int. J. Circuit Theory Appl. 48, 1864–1872. https://doi.org/10.1002/cta.2851.

Bhavanasi, V., Kumar, V., Parida, K., Wang, J., and Lee, P.S. (2016). Enhanced piezoelectric energy harvesting performance of flexible PVDF-TrFE bilayer films with graphene oxide. ACS Appl. Mater. Inter. 8, 521–529. https://doi.org/10.1021/acsami.5b09502.

Cao, R., Pu, X., Du, X., Yang, W., Wang, J., Guo, H., Zhao, S., Yuan, Z., Zhang, C., Li, C., and Wang, Z.L. (2018). Screen-printed washable electronic textiles as self-powered touch/gesture tribo-sensors for intelligent human-machine interaction. ACS Nano 12, 5190–5196. https://doi.org/10.1021/acsnano.8b02477.

Cao, W.T., Ouyang, H., Xin, W., Chao, S., Ma, C., Li, Z., Chen, F., and Ma, M.G. (2020). A stretchable highoutput triboelectric nanogenerator improved by MXene liquid electrode with high electronegativity. Adv. Funct. Mater. 30, 1–10. https://doi.org/10.1002/adfm.202004181.

Carlson, E.J., Strunz, K., and Otis, B.P. (2010). A 20 mV input boost converter with efficient digital control for thermoelectric energy harvesting. IEEE J. Solid-State Circuits. https://doi.org/10.1109/JSSC.2010.2042251.

Chen, X., Li, X., Shao, J., An, N., Tian, H., Wang, C., Han, T., Wang, L., and Lu, B. (2017). High-performance piezoelectric nanogenerators with imprinted P(VDF-TrFE)/BaTiO3 nanocomposite micropillars for self-powered flexible sensors. Small 13, 1–12. https://doi.org/10.1002/smll.201604245.

Chen, B., Yang, Y., and Wang, Z.L. (2018a). Scavenging wind energy by triboelectric nanogenerators. Adv. Energy Mater. 8. https://doi.org/10.1002/aenm.201702649.

Chen, X., Miao, L., Guo, H., Chen, H., Song, Y., Su, Z., and Zhang, X. (2018b). Waterproof and stretchable triboelectric nanogenerator for biomechanical energy harvesting and self-powered sensing. Appl. Phys. Lett. 112, 1–6. https://doi.org/10.1063/1.5028478.

Chen, H., Song, Y., Cheng, X., and Zhang, H. (2019). Self-powered electronic skin based on the triboelectric generator. Nano Energy 56, 252–268. https://doi.org/10.1016/j.nanoen.2018.11.061.

Chen, X., Villa, N.S., Zhuang, Y., Chen, L., Wang, T., Li, Z., and Kong, T. (2020a). Stretchable supercapacitors as emergent energy storage units for health monitoring Bioelectronics. Adv. Energy Mater. 10. https://doi.org/10.1002/aenm.201902769.

Chen, C., Guo, H., Chen, L., Wang, Y.C., Pu, X., Yu, W., Wang, F., Du, Z., and Wang, Z.L. (2020b). Direct current fabric triboelectric nanogenerator for biomotion energy harvesting. ACS Nano 14,

4585–4594. https://doi.org/10.1021/acsnano.0c00138.

Cheng, Y., Lu, X., Chan, K.H., Wang, R., Cao, Z., Sun, J., and Ho, G.W. (2017). A stretchable fiber nanogenerator for versatile mechanical energy harvesting and self-powered full-range personal healthcare monitoring. Nano Energy 41, 511–518. https://doi.org/10.1016/j.nanoen.2017.10.010.

Cheng, X., Tang, W., Song, Y., Chen, H., Zhang, H., and Wang, Z.L. (2019). Power management and effective energy storage of pulsed output from triboelectric nanogenerator. Nano Energy 61, 517–532. https://doi.org/10.1016/j.nanoen.2019.04.096.

Cheng, B., Ma, J., Li, G., Bai, S., Xu, Q., Cui, X., Cheng, L., Qin, Y., and Wang, Z.L. (2020). Mechanically asymmetrical triboelectric nanogenerator for self-powered monitoring of in vivo microscale weak movement. Adv. Energy Mater. 10. https://doi.org/10.1002/aenm.202000827.

Cheng, X. (2019). Power management of triboelectric nanogenerators 5. In 1 Theoretical Analysis of Power Transmittance of TENGs (Wiley Online Library), pp. 77–93.

Cho, H., Chung, J., Shin, G., Sim, J.Y., Kim, D.S., Lee, S., and Hwang, W. (2019). Toward sustainable output generation of liquid–solid contact triboelectric nanogenerators: the role of hierarchical structures. Nano Energy 56, 56–64. https://doi.org/10.1016/j.nanoen.2018.11.039.

Chu, H., Jang, H., Lee, Y., Chae, Y., and Ahn, J.H. (2016). Conformal, graphene-based triboelectric nanogenerator for self-powered wearable electronics. Nano Energy 27, 298–305. https://doi.org/10.1016/j.nanoen.2016.07.009.

Chun, J., Ye, B.U., Lee, J.W., Choi, D., Kang, C.Y., Kim, S.W., Wang, Z.L., and Baik, J.M. (2016). Boosted output performance of triboelectric nanogenerator via electric double layer effect. Nat. Commun. 7, 12985–12989. https://doi.org/10.1038/ncomms12985.

Clare, L.R., and Burrow, S.G. (2008). Power conditioning for energy harvesting. In Active Passive Smart Structures Integrated Systems 2008 (SPIE), pp. 75–87.

Cui, N., Liu, J., Gu, L., Bai, S., Chen, X., and Qin, Y. (2015). Wearable triboelectric generator for powering the portable electronic devices. ACS Appl. Mater. Inter. 7, 18225–18230. https://doi.org/10.1021/am5071688.

D'hulst, R., Sterken, T., Puers, R., and Driesen, J. (2005). Requirements for power electronics used for energy harvesting devices. In PowerMEMS 2005 (University. of Tokyo), pp. 53–56.

Diaz, A.F., and Felix-Navarro, R.M. (2004). A semi-quantitative tribo-electric series for polymeric materials: the influence of chemical structure and properties. J. Electrostat. 62, 277–290. https://doi.org/10.1016/j.elstat.2004.05.005.

Domingos, I., Neves, A.I.S., Craciun, M.F., and Alves, H. (2021). Graphene based triboelectric nanogenerators using water based solution process. Front. Phys. 9, 1–8. https://doi.org/10.3389/fphy.2021.742563.

Dong, K., Deng, J., Zi, Y., Wang, Y.C., Xu, C., Zou, H., Ding, W., Dai, Y., Gu, B., Sun, B., and Wang, Z.L. (2017a). 3D orthogonal woven triboelectric nanogenerator for effective biomechanical energy harvesting and as self-powered active motion sensors. Adv. Mater. 29, 1–11. https://doi.org/10.1002/adma.201702648.

Dong, K., Wang, Y.C., Deng, J., Dai, Y., Zhang, S.L., Zou, H., Gu, B., Sun, B., and Wang, Z.L. (2017b). A highly stretchable and washable all-yarn-based self-charging knitting power textile composed of fiber triboelectric nanogenerators and supercapacitors. ACS Nano. https://doi.org/10.1021/acsnano.7b05317.

Dudem, B., Kim, D.H., Bharat, L.K., and Yu, J.S. (2018). Highly-flexible piezoelectric nanogenerators with silver nanowires and barium titanate embedded composite films for mechanical energy harvesting. Appl. Energy 230, 865–874. https://doi.org/10.1016/j.apenergy.2018.09.009.

Fan, F.R., Tian, Z.Q., and Lin Wang, Z. (2012a). Flexible triboelectric generator. Nano Energy 1, 328–334. https://doi.org/10.1016/j.nanoen.2012.01.004.

Fan, F.R., Lin, L., Zhu, G., Wu, W., Zhang, R., and Wang, Z.L. (2012b). Transparent triboelectric nanogenerators and self-powered pressure sensors based on micropatterned plastic films. Nano Lett. 12, 3109–3114. https://doi.org/10.1021/nl300988z.

Fan, W., He, Q., Meng, K., Tan, X., Zhou, Z., Zhang, G., Yang, J., and Wang, Z.L. (2020). Machine-knitted washable sensor array textile for precise epidermal physiological signal monitoring. Sci. Adv. 6, eaay2840. https://doi.org/10.1126/sciadv.aay2840.

Fang, Z., Chan, K.H., Lu, X., Tan, C.F., and Ho, G.W. (2017). Surface texturing and dielectric property tuning toward boosting of triboelectric nanogenerator performance. J. Mater. Chem. A. 6, 52–57. https://doi.org/10.1039/c7ta07696g.

Feng, X., Li, Q., and Wang, K. (2021). Waste plastic triboelectric nanogenerators using recycled plastic bags for power generation. ACS Appl. Mater. Inter. 13, 400–410. https://doi.org/10.1021/acsami.0c16489.

Ghaffarinejad, A., Hasani, J.Y., Hinchet, R., Lu, Y., Zhang, H., Karami, A., Galayko, D., Kim, S.W., and Basset, P. (2018). A conditioning circuit with exponential enhancement of output energy for triboelectric nanogenerator. Nano Energy 51, 173–184. https://doi.org/10.1016/j.nanoen.2018.06.034.

Gong, W., Hou, C., Guo, Y., Zhou, J., Mu, J., Li, Y., Zhang, Q., and Wang, H. (2017). A wearable, fibroid, self-powered active kinematic sensor based on stretchable sheath-core structural triboelectric fibers. Nano Energy 39, 673–683. https://doi.org/10.1016/j.nanoen.2017.08.003.

Guan, X., Xu, B., Wu, M., Jing, T., Yang, Y., and Gao, Y. (2021). Breathable, washable and wearable woven-structured triboelectric nanogenerators utilizing electrospun nanofibers for biomechanical energy harvesting and self-powered sensing. Nano Energy 80, 105549. https://doi.org/10.1016/j.nanoen.2020.105549.

Guo, H., Chen, J., Yeh, M.H., Fan, X., Wen, Z., Li, Z., Hu, C., and Wang, Z.L. (2015). An ultrarobust high-performance triboelectric nanogenerator based on charge replenishment. ACS Nano 9, 5577–5584. https://doi.org/10.1021/acsnano.5b01830.

Guo, Y., Li, K., Hou, C., Li, Y., Zhang, Q., and Wang, H. (2016). Fluoroalkylsilane-modified textile-based personal energy management device for multifunctional wearable applications. ACS Appl. Mater. Inter. 8, 4676–4683. https://doi.org/10.1021/acsami.5b11622.

Guo, H., Yeh, M.H., Zi, Y., Wen, Z., Chen, J., Liu, G., Hu, C., and Wang, Z.L. (2017). Ultralight cut-paper-based self-charging power unit for self-powered portable electronic and medical systems. ACS Nano 11, 4475–4482. https://doi.org/10.1021/acsnano.7b00866.

Haque, R.I., Farine, P.A., and Briand, D. (2018). Soft triboelectric generators by use of cost-effective elastomers and simple casting process. Sens. Actuators A. Phys. 271, 88–95. https://doi.org/10.1016/j.sna.2017.12.018.

Hashemi, S., Sawan, M., and Savaria, Y. (2009). A novel low-drop CMOS active rectifier for RF-powered devices: experimental results. Microelectron. J. https://doi.org/10.1016/j.mejo.2009.02.007.

He, T., Shi, Q., Wang, H., Wen, F., Chen, T., Ouyang, J., and Lee, C. (2019). Beyond energy harvesting - multi-functional triboelectric nanosensors on a textile. Nano Energy 57, 338–352. https://doi.org/10.1016/j.nanoen.2018.12.032.

Hinchet, R., Ghaffarinejad, A., Lu, Y., Hasani, J.Y., Kim, S.W., and Basset, P. (2018). Understanding and modeling of triboelectric-electret nanogenerator. Nano Energy. https://doi.org/10.1016/j.nanoen.2018.02.030.

Hinchet, R., Seung, W., and Kim, S.W. (2015). Recent progress on flexible triboelectric nanogenerators for SelfPowered electronics. ChemSusChem 8, 2327–2344. https://doi.org/10.1002/cssc.201403481.

Hou, T.C., Yang, Y., Zhang, H., Chen, J., Chen, L.J., and Wang, Z.L. (2013a). Triboelectric nanogenerator built inside shoe insole for harvesting walking energy. Nano Energy 2, 856–862. https://doi.org/10.1016/j.nanoen.2013.03.001.

Hou, C., Huang, T., Wang, H., Yu, H., Zhang, Q., and Li, Y. (2013b). A strong and stretchable self-healing film with self-activated pressure sensitivity for potential artificial skin applications. Sci. Rep. 3, 3138–3225. https://doi.org/10.1038/srep03138.

Hu, J., and Min, H. (2005). A low power and high performance analog front end for passive RFID transponder. In Proceedings - Fourth IEEE Workshop on Automatic Identification Advanced Technologies, AUTO ID 2005. https://doi.org/10.1109/AUTOID.2005.4.

Hu, Y., and Sun, X. (2014). Flexible rechargeable lithium ion batteries: advances and challenges in materials and process technologies. J. Mater. Chem. A. https://doi.org/10.1039/c4ta00716f.

Hwang, H.J., Yeon, J.S., Jung, Y., Park, H.S., and Choi, D. (2020). Extremely foldable and highly porous reduced graphene oxide films for shape-adaptive triboelectric nanogenerators. Small. https://doi.org/10.1002/smll.201903089.

Jiang, D., Ouyang, H., Shi, B., Zou, Y., Tan, P., Qu, X., Shengyu, C., Xi, Y., Zhao, C., Fan, Y., et al. (2020). A wearable noncontact free-rotating hybrid nanogenerator for self-powered electronics. InfoMat 2, 1191–1200. https://doi.org/10.1002/inf2.12103.

Jing, Q., Zhu, G., Bai, P., Xie, Y., Chen, J., Han, R.P., and Wang, Z.L. (2014). Case-encapsulated triboelectric nanogenerator for harvesting energy from reciprocating sliding motion. ACS Nano 8, 3836–3842. https://doi.org/10.1021/nn500694y.

Jost, K., Stenger, D., Perez, C.R., McDonough, J.K., Lian, K., Gogotsi, Y., and Dion, G. (2013). Knitted and screen printed carbon-fiber supercapacitors for applications in wearable electronics. Energy Environ. Sci. https://doi.org/10.1039/c3ee40515j.

Jung, S., Lee, J., Hyeon, T., Lee, M., and Kim, D.H. (2014). Fabric-based integrated energy devices for wearable activity monitors. Adv. Mater. 26, 6329–6334. https://doi.org/10.1002/adma.201402439.

Kang, J.H., Jeong, D.K., and Ryu, S.W. (2017). Transparent, flexible piezoelectric nanogenerator based on GaN membrane using electrochemical lift-off. ACS Appl. Mater. Inter. 9, 10637–10642. https://doi.org/10.1021/acsami.6b15587.

Khan, S.A., Zhang, H.L., Xie, Y., Gao, M., Shah, M.A., Qadir, A., and Lin, Y. (2017). Flexible triboelectric nanogenerator based on carbon nanotubes for self-powered weighing. Adv. Eng. Mater. 19, 1–7. https://doi.org/10.1002/adem.201600710.

Kim, D.H., Viventi, J., Amsden, J.J., Xiao, J., Vigeland, L., Kim, Y.S., Blanco, J.A., Panilaitis, B., Frechette, E.S., Contreras, D., et al. (2010). Dissolvable films of silk fibroin for ultrathin conformal bio-integrated electronics. Nat. Mater. 9, 511–517. https://doi.org/10.1038/nmat2745.

Kim, K., Song, G., Park, C., and Yun, K.S. (2017). Multifunctional woven structure operating as triboelectric energy harvester, capacitive tactile sensor array, and piezoresistive strain sensor array. Sensors (Basel) 17. https://doi.org/10.3390/s17112582.

Ko, Y.H., Nagaraju, G., and Yu, J.S. (2015). Multi-stacked PDMS-based triboelectric generators with conductive textile for efficient energy harvesting. RSC Adv. 5, 6437–6442. https://doi.org/10.1039/c4ra15310c.

Kong, N., Cochran, T., Ha, D.S., Lin, H.C., and Inman, D.J. (2010). A self-power power management circuit for energy harvested by a piezoelectric cantilever. In Conference Proceedings - IEEE Applied Power Electronics Conference and Exposition - APEC. https://doi.org/10.1109/APEC.2010.5433535.

Lai, Y.C., Deng, J., Zhang, S.L., Niu, S., Guo, H., and Wang, Z.L. (2017). Single-thread-based wearable and highly stretchable triboelectric nanogenerators and their applications in cloth-based self-powered human-interactive and

biomedical sensing. Adv. Funct. Mater. 27, 1–10. https://doi.org/10.1002/adfm.201604462.

Lallart, M., and Guyomar, D. (2008). An optimized self-powered switching circuit for non-linear energy harvesting with low voltage output. Smart Mater. Struct. https://doi.org/10.1088/0964-1726/17/3/035030.

Lam, Y.H., Ki, W.H., and Tsui, C.Y. (2006). Integrated low-loss CMOS active rectifier for wireless powered devices. IEEE Trans. Circuits Syst. Express Briefs. https://doi.org/10.1109/TCSII.2006.885400.

Le, T.T., Han, J., Von Jouanne, A., Mayaram, K., and Fiez, T.S. (2006). Piezoelectric micro-power generation interface circuits. IEEE J. Solid-State Circuits. https://doi.org/10.1109/JSSC.2006.874286.

Lee, J.W., Ye, B.U., and Baik, J.M. (2017). Research Update: recent progress in the development of effective dielectrics for high-output triboelectric nanogenerator. APL Mater. 5. https://doi.org/10.1063/1.4979306.

Lefeuvre, E., Audigier, D., Richard, C., and Guyomar, D. (2007). Buck-boost converter for sensorless power optimization of piezoelectric energy harvester. IEEE Trans. Power Electron. https://doi.org/10.1109/TPEL.2007.904230.

Lehmann, T., and Moghe, Y. (2005). On-chip active power rectifiers for biomedical applications. In Proceedings - IEEE International Symposium on Circuits and Systems. https://doi.org/10.1109/ISCAS.2005.1464692.

Lewandowski, A., Jakobczyk, P., Galinski, M., and Biegun, M. (2013). Self-discharge of electrochemical double layer capacitors. Phys. Chem. Chem. Phys. https://doi.org/10.1039/c3cp44612c.

Li, Y., Cheng, G., Lin, G.H., Yang, J., Lin, L., and Wang, Z.L. (2015). Single-electrode-based rotatory triboelectric nanogenerator and its applications as self-powered contact area and eccentric angle sensors. Nano Energy 11, 323–332. https://doi.org/10.1016/j.nanoen.2014.11.010.

Li, X., and Sun, Y. (2017). WearETE: a scalable wearable E-textile triboelectric energy harvesting system for human motion scavenging. Sensors (Basel) 17. https://doi.org/10.3390/s17112649.

Li, W., Torres, D., Wang, T., Wang, C., and Sepúlveda, N. (2016). Flexible and biocompatible polypropylene ferroelectret nanogenerator (FENG): on the path toward wearable devices powered by human motion. Nano Energy 30, 649–657. https://doi.org/10.1016/j.nanoen.2016.10.007.

Li, H., Zhang, X., Zhao, L., Jiang, D., Xu, L., Liu, Z., Wu, Y., Hu, K., Zhang, M.R., Wang, J., et al. (2020). A hybrid biofuel and triboelectric nanogenerator for bioenergy harvesting. Nanomicro Lett. 12. https://doi.org/10.1007/s40820-020-0376-8.

Lin, P.M., and Chua, L.O. (1977). Topological generation and analysis of voltage multiplier circuits. IEEE Trans. Circuits Syst. https://doi.org/10.1109/TCS.1977.1084273.

Lin, L., Wang, S., Niu, S., Liu, C., Xie, Y., and Wang, Z.L. (2014). Noncontact free-rotating disk

triboelectric nanogenerator as a sustainable energy harvester and self-powered mechanical sensor. ACS Appl. Mater. Inter. 6, 3031–3038. https://doi.org/10.1021/am405637s.

Lin, Z., Chen, J., Li, X., Zhou, Z., Meng, K., Wei, W., Yang, J., and Wang, Z.L. (2017). Triboelectric nanogenerator enabled body sensor network for self-powered human heart-rate monitoring. ACS Nano 11, 8830–8837. https://doi.org/10.1021/acsnano.7b02975.

Liu, L., Pan, J., Chen, P., Zhang, J., Yu, X., Ding, X., Wang, B., Sun, X., and Peng, H. (2016). A triboelectric textile templated by a three-dimensionally penetrated fabric. J. Mater. Chem. A. 4, 6077–6083. https://doi.org/10.1039/c6ta01166g.

Liu, S., Zheng, W., Yang, B., and Tao, X. (2018). Triboelectric charge density of porous and deformable fabrics made from polymer fibers. Nano Energy 53, 383–390. https://doi.org/10.1016/j.nanoen.2018.08.071.

Liu, W., Wang, Z., Wang, G., Liu, G., Chen, J., Pu, X., Xi, Y., Wang, X., Guo, H., Hu, C., and Wang, Z.L. (2019). Integrated charge excitation triboelectric nanogenerator. Nat. Commun. 10, 1426. https://doi.org/10.1038/s41467-019-09464-8.

Liu, L., Yang, X., Zhao, L., Xu, W., Wang, J., Yang, Q., and Tang, Q. (2020). Nanowrinkle-patterned flexible woven triboelectric nanogenerator toward self-powered wearable electronics. Nano Energy 73. https://doi.org/10.1016/j.nanoen.2020.104797.

Lou, M., Abdalla, I., Zhu, M., Wei, X., Yu, J., Li, Z., and Ding, B. (2020). Highly wearable, breathable, and washable sensing textile for human motion and pulse monitoring. ACS Appl. Mater. Inter. 12, 19965–19973. https://doi.org/10.1021/acsami.0c03670.

Lu, Y., O'Riordan, E., Cottone, F., Boisseau, S., Galayko, D., Blokhina, E., Marty, F., and Basset, P. (2016). A batch-fabricated electret-biased wideband MEMS vibration energy harvester with frequency-up conversion behavior powering a UHF wireless sensor node. J. Micromech. Microeng. https://doi.org/10.1088/0960-1317/26/12/124004.

Maria Joseph Raj, N.P., Alluri, N.R., Khandelwal, G., and Kim, S.J. (2019). Lead-free piezoelectric nanogenerator using lightweight composite films for harnessing biomechanical energy. Compos. Part B Eng. 161, 608–616. https://doi.org/10.1016/j.compositesb.2018.12.129.

Marinkovic, D., Frey, A., Kuehne, I., and Scholl, G. (2009). A new rectifier and trigger circuit for a piezoelectric microgenerator. Procedia Chem. https://doi.org/10.1016/j.proche.2009.07.361.

Marzencki, M., Ammar, Y., and Basrour, S. (2008). Integrated power harvesting system including a MEMS generator and a power management circuit. Sensors Actuators A. Phys. https://doi.org/10.1016/j.sna.2007.10.073.

McCarty, L.S., and Whitesides, G.M. (2008). Electrostatic charging due to separation of ions at interfaces: contact electrification of ionic electrets. Angew. Chem. Int. Ed. Engl. 47, 2188–2207. https://doi.org/10.1002/anie.200701812.

Niu, S., Liu, Y., Wang, S., Lin, L., Zhou, Y.S., Hu, Y., and Wang, Z.L. (2013a). Theory of sliding-mode triboelectric nanogenerators. Adv. Mater. https://doi.org/10.1002/adma.201302808.

Niu, S., Wang, S., Lin, L., Liu, Y., Zhou, Y.S., Hu, Y., and Wang, Z.L. (2013b). Theoretical study of contact-mode triboelectric nanogenerators as an effective power source. Energy Environ. Sci. 6, 3576–3583. https://doi.org/10.1039/c3ee42571a.

Niu, S., Zhou, Y.S., Wang, S., Liu, Y., Lin, L., Bando, Y., and Wang, Z.L. (2014a). Simulation method for optimizing the performance of an integrated triboelectric nanogenerator energy harvesting system. Nano Energy 8, 150–156. https://doi.org/10.1016/j.nanoen.2014.05.018.

Niu, S., Wang, S., Liu, Y., Zhou, Y.S., Lin, L., Hu, Y., Pradel, K.C., and Wang, Z.L. (2014b). A theoretical study of grating structured triboelectric nanogenerators. Energy Environ. Sci. 7, 2339–2349. https://doi.org/10.1039/c4ee00498a.

Niu, S., and Wang, Z.L. (2014). Theoretical systems of triboelectric nanogenerators. Nano Energy 14, 161–192. https://doi.org/10.1016/j.nanoen.2014.11.034.

Niu, S., Wang, X., Yi, F., Zhou, Y.S., and Wang, Z.L. (2015). A universal self-charging system driven by random biomechanical energy for sustainable operation of mobile electronics. Nat. Commun. https://doi.org/10.1038/ncomms9975.

Ostfeld, A.E., Gaikwad, A.M., Khan, Y., and Arias, A.C. (2016). High-performance flexible energy storage and harvesting system for wearable electronics. Sci. Rep. https://doi.org/10.1038/srep26122.

Ouyang, H., Liu, Z., Li, N., Shi, B., Zou, Y., Xie, F., Ma, Y., Li, Z., Li, H., Zheng, Q., et al. (2019). Symbiotic cardiac pacemaker. Nat. Commun. 10, 1821–1910. https://doi.org/10.1038/s41467-019-09851-1.

Park, C.H., Park, J.K., Jeon, H.S., and Chun, B.C. (2008). Triboelectric series and charging properties of plastics using the designed vertical-reciprocation charger. J. Electrostat. 66, 578–583. https://doi.org/10.1016/j.elstat.2008.07.001.

Peters, C., Kessling, O., Henrici, F., Ortmanns, M., and Manoli, Y. (2007). CMOS integrated highly efficient full wave rectifier. In Proceedings - IEEE International Symposium on Circuits and Systems. https://doi.org/10.1109/iscas.2007.377947.

Peters, C., Henrici, F., Ortmanns, M., and Manoli, Y. (2008). High-bandwidth floating gate CMOS rectifiers with reduced voltage drop. In Proceedings - IEEE International Symposium on Circuits and Systems. https://doi.org/10.1109/ISCAS.2008.4541988.

Prauzek, M., Konecny, J., Borova, M., Janosova, K., Hlavica, J., and Musilek, P. (2018). Energy harvesting sources, storage devices and system topologies for environmental wireless sensor networks: a review. Sensors. https://doi.org/10.3390/s18082446.

Pu, X., Li, L., Liu, M., Jiang, C., Du, C., Zhao, Z., Hu, W., and Wang, Z.L. (2016a). Wearable self-charging power textile based on flexible yarn supercapacitors and fabric nanogenerators. Adv.

Mater. 28, 98–105. https://doi.org/10.1002/adma.201504403.

Pu, X., Song, W., Liu, M., Sun, C., Du, C., Jiang, C., Huang, X., Zou, D., Hu, W., and Wang, Z.L. (2016b). Wearable power-textiles by integrating fabric triboelectric nanogenerators and fiber-shaped dye-sensitized solar cells. Adv. Energy Mater. 6. https://doi.org/10.1002/aenm.201601048.

Pu, X., Hu, W., and Wang, Z.L. (2018). Toward wearable self-charging power systems: the integration of energy-harvesting and storage devices. Small 14, 1–19. https://doi.org/10.1002/smll.201702817.

Pusty, M., and Shirage, P.M. (2020). Gold nanoparticle-cellulose/PDMS nanocomposite: a flexible dielectric material for harvesting mechanical energy. RSC Adv. 10, 10097–10112. https://doi.org/10.1039/c9ra10811d.

Pyo, S., Kim, M.O., Kwon, D.S., Kim, W., Yang, J.-H., Cho, H.S., Lee, J.H., and Kim, J. (2020). All-textile wearable triboelectric nanogenerator using pile-embroidered fibers for enhancing output power. Smart Mater. Struct. 29. https://doi.org/10.1088/1361-665X/ab710a.

Qiu, J., Jiang, H., Ji, H., and Zhu, K. (2009). Comparison between four piezoelectric energy harvesting circuits. Front. Mech. Eng. China 4, 153–159. https://doi.org/10.1007/s11465-009-0031-z.

Rajasekaran, A., Hande, A., and Bhatia, D. (2008). Buck-boost converter based power conditioning circuit for low. In Third Annu. (studylib.net), pp. 1–3.

Ramadass, Y.K., and Chandrakasan, A.P. (2010a). A batteryless thermoelectric energy-harvesting interface circuit with 35mV startup voltage. In Digest of Technical Papers - IEEE International Solid-State Circuits Conference. https://doi.org/10.1109/ISSCC.2010.5433835.

Ramadass, Y.K., and Chandrakasan, A.P. (2010b). An efficient piezoelectric energy harvesting interface circuit using a bias-flip rectifier and shared inductor. IEEE J. Solid-State Circuits. https://doi.org/10.1109/JSSC.2009.2034442.

Rawy, K., Sharma, R., Yoon, H.J., Khan, U., Kim, S.W., and Kim, T.T. (2018). An 88% efficiency 2.4μW to 15.6μW triboelectric nanogenerator energy harvesting system based on a single-comparator control algorithm. In 2018 IEEE Asian Solid-State Circuits Conference, A-SSCC 2018 - Proceedings. https://doi.org/10.1109/ASSCC.2018.8579338.

Ren, Z., Nie, J., Shao, J., Lai, Q., Wang, L., Chen, J., Chen, X., and Wang, Z.L. (2018). Fully elastic and metal-free tactile sensors for detecting both normal and tangential forces based on triboelectric nanogenerators. Adv. Funct. Mater. 28, 1–9. https://doi.org/10.1002/adfm.201802989.

Rue, B., Levacq, D., and Flandre, D. (2006). Low-voltage low-power high-temperature SOI CMOS rectifiers. In Proceedings - IEEE International SOI Conference. https://doi.org/10.1109/SOI.2006.284435.

Saeid, S., and Aghcheh, H. (2011). High-Efficiency Low-Voltage Rectifiers for Power Scavenging

Systems (École Polytechnique de Montréal), pp. 10–23.

Schneuwly, A., and Gallay, R. (2000). Properties and applications of supercapacitors from the state-of-the-art to future trends. In PCIM2000 (Citeseer), pp. 58–75.

Seeman, M.D., Ng, V.W., Le, H.P., John, M., Alon, E., and Sanders, S.R. (2010). A comparative Analysis of Switched-Capacitor and Inductor-Based DC-DC Conversion Technologies. https://doi.org/10.1109/COMPEL.2010.5562407.

Seol, M., Kim, S., Cho, Y., Byun, K.E., Kim, H., Kim, J., Kim, S.K., Kim, S.W., Shin, H.J., and Park, S. (2018). Triboelectric series of 2D layered materials. Adv. Mater. 30, e1801210. https://doi.org/10.1002/adma.201801210.

Shi, M., Zhang, J., Han, M., Song, Y., Su, Z., and Zhang, H. (2016). A single-electrode wearable triboelectric nanogenerator based on conductive & stretchable fabric. In Proceedings - IEEE International Conference on Micro Electro Mechanical Systems, pp. 1228–1231. https://doi.org/10.1109/MEMSYS.2016.7421859.

Shi, M., Wu, H., Zhang, J., Han, M., Meng, B., and Zhang, X. (2017). Self-powered wireless smart patch for healthcare monitoring. Nano Energy 32, 479–487. https://doi.org/10.1016/j.nanoen.2017.01.008.

Shi, B., Liu, Z., Zheng, Q., Meng, J., Ouyang, H., Zou, Y., Jiang, D., Qu, X., Yu, M., Zhao, L., et al. (2019). Body-integrated self-powered system for wearable and implantable applications. ACS Nano. 13, 6017–6024. https://doi.org/10.1021/acsnano.9b02233.

Shin, D.W., Barnes, M.D., Walsh, K., Dimov, D., Tian, P., Neves, A.I.S., Wright, C.D., Yu, S.M., Yoo, J.B., Russo, S., and Craciun, M.F. (2018). A new facile route to flexible and semi-transparent electrodes based on water exfoliated graphene and their single-electrode triboelectric nanogenerator. Adv. Mater. 30, e1802953. https://doi.org/10.1002/adma.201802953.

Soin, N., Zhao, P., Prashanthi, K., Chen, J., Ding, P., Zhou, E., Shaha, T., Ray, S.C., Tsonos, C., Thundat, T., et al. (2016). High performance triboelectric nanogenerators based on phase-inversion piezoelectric membranes of poly(vinylidene fluoride)-zinc stannate (PVDF-ZnSnO3) and polyamide-6 (PA6). Nano Energy 30, 470–480. https://doi.org/10.1016/j.nanoen.2016.10.040.

Song, G., Kim, Y., Yu, S., Kim, M.O., Park, S.H., Cho, S.M., Velusamy, D.B., Cho, S.H., Kim, K.L., Kim, J., et al. (2015). Molecularly engineered surface triboelectric nanogenerator by self-assembled monolayers (METS). Chem. Mater. 27, 4749–4755. https://doi.org/10.1021/acs.chemmater.5b01507.

Szarka, G.D., Stark, B.H., and Burrow, S.G. (2012). Review of power conditioning for kinetic energy harvesting systems. IEEE Trans. Power Electron. https://doi.org/10.1109/TPEL.2011.2161675.

Sze, N.M., Ki, W.H., and Tsui, C.Y. (2008). Threshold voltage start-up boost converter for sub-mA applications. In Proceedings - 4th IEEE International Symposium on Electronic Design, Test and Applications, DELTA 2008. https://doi.org/10.1109/DELTA.2008.126.

Tabesh, A., and Fréchette, L.G. (2010). A low-power stand-alone adaptive circuit for harvesting energy from a piezoelectric micropower generator. IEEE Trans. Ind. Electron. 57, 840–849. https://doi.org/10.1109/TIE.2009.2037648.

Tian, Z., He, J., Chen, X., Zhang, Z., Wen, T., Zhai, C., Han, J., Mu, J., Hou, X., Chou, X., and Xue, C. (2017). Performance-boosted triboelectric textile for harvesting human motion energy. Nano Energy 39, 562–570. https://doi.org/10.1016/j.nanoen.2017.06.018.

Tian, Z., He, J., Chen, X., Wen, T., Zhai, C., Zhang, Z., Cho, J., Chou, X., and Xue, C. (2018). Core-shell coaxially structured triboelectric nanogenerator for energy harvesting and motion sensing. RSC Adv. 8, 2950–2957. https://doi.org/10.1039/c7ra12739a.

Tse, C.K., Wong, S.C., and Chow, M.H.L. (1995). On lossless switched-capacitor power converters. IEEE Trans. Power Electron. https://doi.org/10.1109/63.387993.

Viallet, F., and Cedex, G. (2006). Non-linear techniques for increasing harvesting energy from piezoelectric and electromagnetic micro-power-generators. Energy, 344–348.

Wang, S., Zi, Y., Zhou, Y.S., Li, S., Fan, F., Lin, L., and Wang, Z.L. (2016). Molecular surface functionalization to enhance the power output of triboelectric nanogenerators. J. Mater. Chem. A. 4, 3728–3734. https://doi.org/10.1039/c5ta10239a.

Wang, W., Zhang, J., Zhang, Y., Chen, F., Wang, H., Wu, M., Li, H., Zhu, Q., Zheng, H., and Zhang, R. (2020a). Remarkably enhanced hybrid piezo/triboelectric nanogenerator via rational modulation of piezoelectric and dielectric properties for self-powered electronics. Appl. Phys. Lett. 116, 1–6. https://doi.org/10.1063/1.5134100.

Wang, X., Zheng, S., Zhou, F., Qin, J., Shi, X., Wang, S., Sun, C., Bao, X., and Wu, Z.S. (2020b). Scalable fabrication of printed Zn//MnO2 planar micro-batteries with high volumetric energy density and exceptional safety. Natl. Sci. Rev. https://doi.org/10.1093/nsr/nwz070.

Wang, S., Lin, L., and Wang, Z.L. (2012). Nanoscale triboelectric-effect-enabled energy conversion for sustainably powering portable electronics. Nano Lett. 12, 6339–6346. https://doi.org/10.1021/nl303573d.

Wang, S., Lin, L., Xie, Y., Jing, Q., Niu, S., and Wang, Z.L. (2013). Sliding-triboelectric nanogenerators based on in-plane charge-separation mechanism. Nano Lett. 13, 2226–2233. https://doi.org/10.1021/nl400738p.

Wang, S., Xie, Y., Niu, S., Lin, L., and Wang, Z.L. (2014a). Freestanding triboelectric-layer-based nanogenerators for harvesting energy from a moving object or human motion in contact and non-contact modes. Adv. Mater. 26, 2818–2824. https://doi.org/10.1002/adma.201305303.

Wang, S., Xie, Y., Niu, S., Lin, L., Liu, C., Zhou, Y.S., and Wang, Z.L. (2014b). Maximum surface charge density for triboelectric nanogenerators achieved by ionized-air injection: methodology and theoretical understanding. Adv. Mater. 26, 6720–6728. https://doi.org/10.1002/adma.201402491.

Wang, S., Lin, L., and Wang, Z.L. (2015a). Triboelectric nanogenerators as self-powered active sensors. Nano Energy 11, 436–462. https://doi.org/10.1016/j.nanoen.2014.10.034.

Wang, S., Mu, X., Wang, X., Gu, A.Y., Wang, Z.L., and Yang, Y. (2015b). Elasto-aerodynamics-driven triboelectric nanogenerator for scavenging air-flow energy. ACS Nano 9, 9554–9563. https://doi.org/10.1021/acsnano.5b04396.

Wang, J., Wu, C., Dai, Y., Zhao, Z., Wang, A., Zhang, T., and Wang, Z.L. (2017). Achieving ultrahigh triboelectric charge density for efficient energy harvesting. Nat. Commun. 8, 88. https://doi.org/10.1038/s41467-017-00131-4.

Wang, Z.L. (2013). Triboelectric nanogenerators as new energy technology for self-powered systems and as active mechanical and chemical sensors. ACS Nano 7, 9533–9557. https://doi.org/10.1021/nn404614z.

Wang, Z.L. (2014). Triboelectric nanogenerators as new energy technology and self-powered sensors - principles, problems and perspectives. Faraday Discuss. 176, 447–458. https://doi.org/10.1039/c4fd00159a.

Wen, R., Guo, J., Yu, A., Zhang, K., Kou, J., Zhu, Y., Zhang, Y., Li, B.W., and Zhai, J. (2018). Remarkably enhanced triboelectric nanogenerator based on flexible and transparent monolayer titania nanocomposite. Nano Energy 50, 140–147. https://doi.org/10.1016/j.nanoen.2018.05.037.

Wu, J.M., Chang, C.K., and Chang, Y.T. (2016). High-output current density of the triboelectric nanogenerator made from recycling rice husks. Nano Energy 19, 39–47. https://doi.org/10.1016/j.nanoen.2015.11.014.

Wu, C., Wang, A.C., Ding, W., Guo, H., and Wang, Z.L. (2019). Triboelectric nanogenerator: a foundation of the energy for the new era. Adv. Energy Mater. 9, 1–25. https://doi.org/10.1002/aenm.201802906.

Wu, M., Gao, Z., Yao, K., Hou, S., Liu, Y., Li, D., He, J., Huang, X., Song, E., Yu, J., et al. (2021). Thin, soft, skin-integrated foam based triboelectric nanogenerators for tactile sensing and energy harvesting. Mater. Today Energy 20, 100657. https://doi.org/10.1016/j.mtener.2021.100657.

Xi, F., Pang, Y., Li, W., Jiang, T., Zhang, L., Guo, T., Liu, G., Zhang, G., and Wang, Z.L. (2017). Universal power management strategy for triboelectric nanogenerator. Nano Energy 37, 168–176. https://doi.org/10.1016/J.NANOEN.2017.05.027.

Xu, S., Ngo, K.D.T., Nishida, T., Chung, G.B., and Sharma, A. (2007). Low frequency pulsed resonant converter for energy harvesting. IEEE Trans. Power Electron. 22, 63–68. https://doi.org/10.1109/TPEL.2006.886647.

Xu, W., Huang, L.B., and Hao, J. (2017). Fully self-healing and shape-tailorable triboelectric nanogenerators based on healable polymer and magnetic-assisted electrode. Nano Energy 40, 399–407. https://doi.org/10.1016/j.nanoen.2017.08.045.

Xu, L., Bu, T.Z., Yang, X.D., Zhang, C., and Wang, Z.L. (2018a). Ultrahigh charge density realized by charge pumping at ambient conditions for triboelectric nanogenerators. Nano Energy 49,

625–633. https://doi.org/10.1016/j.nanoen.2018.05.011.

Xu, C., Zi, Y., Wang, A.C., Zou, H., Dai, Y., He, X., Wang, P., Wang, Y.C., Feng, P., Li, D., and Wang, Z.L. (2018b). On the electron-transfer mechanism in the contact-electrification effect. Adv. Mater. 30, e1706790. https://doi.org/10.1002/adma.201706790.

Xu, W., Wong, M.C., and Hao, J. (2019). Strategies and progress on improving robustness and reliability of triboelectric nanogenerators. Nano Energy 55, 203–215. https://doi.org/10.1016/j.nanoen.2018.10.073.

Yan, S., Lu, J., Song, W., and Xiao, R. (2018). Flexible triboelectric nanogenerator based on cost-effective thermoplastic polymeric nanofiber membranes for body-motion energy harvesting with high humidity-resistance. Nano Energy 48, 248–255. https://doi.org/10.1016/j.nanoen.2018.03.031.

Yang, W., Chen, J., Zhu, G., Wen, X., Bai, P., Su, Y., Lin, Y., and Wang, Z. (2013). Harvesting vibration energy by a triple-cantilever based triboelectric nanogenerator. Nano Res. 6, 880–886. https://doi.org/10.1007/s12274-013-0364-0.

Yang, Y., Yuan, W., Zhang, X., Yuan, Y., Wang, C., Ye, Y., Huang, Y., Qiu, Z., and Tang, Y. (2020). Overview on the applications of three-dimensional printing for rechargeable lithium-ion batteries. Appl. Energy. https://doi.org/10.1016/j.apenergy.2019.114002.

Yang, Y., Zhang, H., Chen, J., Jing, Q., Zhou, Y.S., Wen, X., and Wang, Z.L. (2013). Single-electrode-based sliding triboelectric nanogenerator for self-powered displacement vector sensor system. ACS Nano. 7, 7342–7351. https://doi.org/10.1021/nn403021m.

Yang, Y., Xie, L., Wen, Z., Chen, C., Chen, X., Wei, A., Cheng, P., Xie, X., and Sun, X. (2018). Coaxial triboelectric nanogenerator and supercapacitor fiber-based self-charging power fabric. ACS Appl. Mater. Inter. 10, 42356–42362. https://doi.org/10.1021/acsami.8b15104.

Ye, S., Cheng, C., Chen, X., Chen, X., Shao, J., Zhang, J., Hu, H., Tian, H., Li, X., Ma, L., and Jia, W. (2019). High-performance piezoelectric nanogenerator based on microstructured P(VDF-TrFE)/BNNTs composite for energy harvesting and radiation protection in space. Nano Energy 60, 701–714. https://doi.org/10.1016/j.nanoen.2019.03.096.

Yi, F., Lin, L., Niu, S., Yang, P.K., Wang, Z., Chen, J., Zhou, Y., Zi, Y., Wang, J., Liao, Q., et al. (2015). Stretchable-rubber-based triboelectric nanogenerator and its application as self-powered body motion sensors. Adv. Funct. Mater. 25, 3688–3696. https://doi.org/10.1002/adfm.201500428.

Yoon, H.J., Ryu, H., and Kim, S.W. (2018). Sustainable powering triboelectric nanogenerators: approaches and the path towards efficient use. Nano Energy 51, 270–285. https://doi.org/10.1016/j.nanoen.2018.06.075.

Yu, Y., Sun, H., Orbay, H., Chen, F., England, C.G., Cai, W., and Wang, X. (2016). Biocompatibility and in vivo operation of implantable mesoporous

PVDF-based nanogenerators. Nano Energy 27, 275–281. https://doi.org/10.1016/j.nanoen.2016.07.015.

Yu, H., He, X., Ding, W., Hu, Y., Yang, D., Lu, S., Wu, C., Zou, H., Liu, R., Lu, C., et al. (2017a). A self-powered dynamic displacement monitoring system based on triboelectric accelerometer. Adv. Energy Mater. 7. https://doi.org/10.1002/aenm.201700565.

Yu, A., Pu, X., Wen, R., Liu, M., Zhou, T., Zhang, K., Zhang, Y., Zhai, J., Hu, W., and Wang, Z.L. (2017b). Core-Shell-yarn-based triboelectric nanogenerator textiles as power cloths. ACS Nano. 11, 12764–12771. https://doi.org/10.1021/acsnano.7b07534.

Yu, A., Zhu, Y., Wang, W., and Zhai, J. (2019). Progress in triboelectric materials: toward high performance and widespread applications. Adv. Funct. Mater. 29, 1900098. https://doi.org/10.1002/adfm.201900098.

Zhang, H., Yang, Y., Hou, T.C., Su, Y., Hu, C., and Wang, Z.L. (2013a). Triboelectric nanogenerator built inside clothes for self-powered glucose biosensors. Nano Energy 2, 1019–1024. https://doi.org/10.1016/j.nanoen.2013.03.024.

Zhang, X.S., Han, M.D., Wang, R.X., Zhu, F.Y., Li, Z.H., Wang, W., and Zhang, H.X. (2013b). Frequency-multiplication high-output triboelectric nanogenerator for sustainably powering biomedical microsystems. Nano Lett. 13, 1168–1172. https://doi.org/10.1021/nl3045684.

Zhang, Q., Liang, Q., Liao, Q., Yi, F., Zheng, X., Ma, M., Gao, F., and Zhang, Y. (2017). Service behavior of multifunctional triboelectric nanogenerators. Adv. Mater. 29. https://doi.org/10.1002/adma.201606703.

Zhang, H., Lu, Y., Ghaffarinejad, A., and Basset, P. (2018). Progressive contact-separate triboelectric nanogenerator based on conductive polyurethane foam regulated with a Bennet doubler conditioning circuit. Nano Energy 51, 10–18. https://doi.org/10.1016/j.nanoen.2018.06.038.

Zhang, P., Chen, Y., Guo, Z.H., Guo, W., Pu, X., Wang, Z.L., et al. (2020). Stretchable, transparent, and thermally stable triboelectric nanogenerators based on solvent-free ion-conducting elastomer electrodes. Adv. Funct. Mater. 30, 1–9. https://doi.org/10.1002/adfm.201909252.

Zheng, Q., Jin, Y., Liu, Z., Ouyang, H., Li, H., Shi, B., Jiang, W., Zhang, H., Li, Z., and Wang, Z.L. (2016). Robust multilayered encapsulation for high-performance triboelectric nanogenerator in harsh environment. ACS Appl. Mater. Inter. 8, 26697–26703. https://doi.org/10.1021/acsami.6b06866.

Zhou, T., Zhang, C., Han, C.B., Fan, F.R., Tang, W., and Wang, Z.L. (2014). Woven structured triboelectric nanogenerator for wearable devices. ACS Appl. Mater. Inter. 6, 14695–14701. https://doi.org/10.1021/am504110u.

Zhou, M., Al-Furjan, M.S.H., Zou, J., and Liu, W. (2018a). A review on heat and mechanical energy harvesting from human – principles, prototypes and perspectives. Renew. Sustain. Energy Rev. 82,

3582–3609. https://doi.org/10.1016/j.rser.2017.10.102.

Zhou, C., Yang, Y., Sun, N., Wen, Z., Cheng, P., Xie, X., Shao, H., Shen, Q., Chen, X., Liu, Y., et al. (2018b). Flexible self-charging power units for portable electronics based on folded carbon paper. Nano Res. 11, 4313–4322. https://doi.org/10.1007/s12274-018-2018-8.

Zhou, Q., Lee, K., Kim, K.N., Park, J.G., Pan, J., Bae, J., Baik, J.M., and Kim, T. (2019). High humidity- and contamination-resistant triboelectric nanogenerator with superhydrophobic interface. Nano Energy 57, 903–910. https://doi.org/10.1016/j.nanoen.2018.12.091.

Zhu, M., Huang, Y., Ng, W.S., Liu, J., Wang, Z., Wang, Z., Hu, H., and Zhi, C. (2016). 3D spacer fabric based multifunctional triboelectric nanogenerator with great feasibility for mechanized large-scale production. Nano Energy 27, 439–446. https://doi.org/10.1016/j.nanoen.2016.07.016.

Zhu, G., Pan, C., Guo, W., Chen, C.Y., Zhou, Y., Yu, R., and Wang, Z.L. (2012). Triboelectric-generator-driven pulse electrodeposition for micropatterning. Nano Lett. 12, 4960–4965. https://doi.org/10.1021/nl302560k.

Zhu, G., Bai, P., Chen, J., and Lin Wang, Z. (2013a). Power-generating shoe insole based on triboelectric nanogenerators for self-powered consumer electronics. Nano Energy 2, 688–692. https://doi.org/10.1016/j.nanoen.2013.08.002.

Zhu, G., Lin, Z.H., Jing, Q., Bai, P., Pan, C., Yang, Y., Zhou, Y., and Wang, Z.L. (2013b). Toward large-scale energy harvesting by a nanoparticle-enhanced triboelectric nanogenerator. Nano Lett. 13, 847–853. https://doi.org/10.1021/nl4001053.

Zhu, G., Chen, J., Zhang, T., Jing, Q., and Wang, Z.L. (2014a). Radial-arrayed rotary electrification for high performance triboelectric generator. Nat. Commun. https://doi.org/10.1038/ncomms4426.

Zhu, G., Yang, W.Q., Zhang, T., Jing, Q., Chen, J., Zhou, Y.S., Bai, P., and Wang, Z.L. (2014b). Self-powered, ultrasensitive, flexible tactile sensors based on contact electrification. Nano Lett. 14, 3208–3213. https://doi.org/10.1021/nl5005652.

Zi, Y., Niu, S., Wang, J., Wen, Z., Tang, W., and Wang, Z.L. (2015). Standards and figure-of-merits for quantifying the performance of triboelectric nanogenerators. Nat. Commun. 6, 8376. https://doi.org/10.1038/ncomms9376.

Zou, Y., Tan, P., Shi, B., Ouyang, H., Jiang, D., Liu, Z., Li, H., Yu, M., Wang, C., Qu, X., et al. (2019a). A bionic stretchable nanogenerator for underwater sensing and energy harvesting. Nat. Commun. 10, 2695–2710. https://doi.org/10.1038/s41467-019-10433-4.

Zou, H., Zhang, Y., Guo, L., Wang, P., He, X., Dai, G., Zheng, H., Chen, C., Wang, A.C., Xu, C., and Wang, Z.L. (2019b). Quantifying the triboelectric series. Nat. Commun. 10, 1427–1429. https://doi.org/10.1038/s41467-019-09461-x.